

AD-A147 049

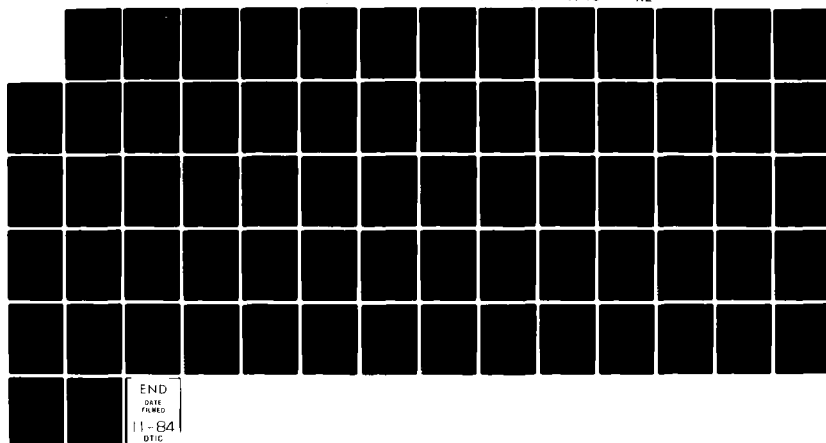
EVALUATION OF THE KORT NOZZLE DESIGN FOR THE UNITED
STATES COAST GUARD 140 WYTM CUTTER(U) NAVAL ACADEMY
ANNAPOLIS MD DIV OF ENGINEERING AND WEAPONS T J LANGAN

UNCLASSIFIED

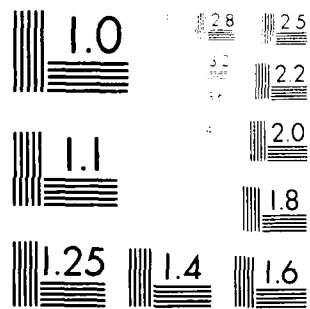
1984 USNA-EW-15-84

1/1

F/G 13/10 NL



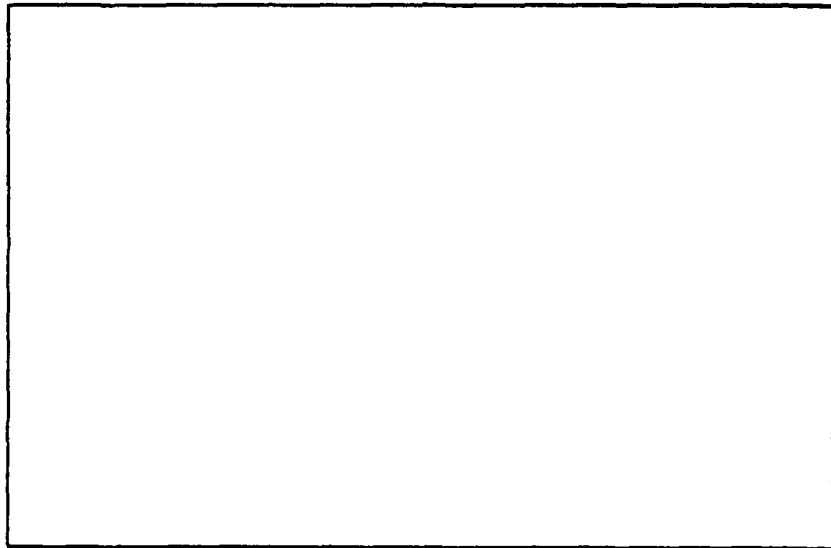
END
PAGE
FWD
11-84
DTIG



MICROCOPY RESOLUTION TEST CHART
NATIONAL BUREAU OF STANDARDS 1963

AD-A147 049

20



UNITED STATES NAVAL ACADEMY
DIVISION OF
ENGINEERING AND WEAPONS
ANNAPOLIS, MARYLAND

DTIC
ELECTED
S NOV 5 1984 D
D

Approved for public release
Distribution Unlimited

84 10 30 138

UNITED STATES NAVAL ACADEMY
Annapolis, Maryland 21402

DIVISION OF ENGINEERING AND MATHEMATICS

REPORT NO. E-1886

EVALUATION OF THE

KORT NOZZLE DESIGN FOR THE

UNITED STATES COAST GUARD

150' WHTM CUTTER

BY

THOMAS J. LANGAS, PH.D.

Professor
Naval Systems Engineering Department
U. S. Naval Academy
Annapolis, Maryland

Accession For	
NTIS CRA&I	<input checked="" type="checkbox"/>
DTIC TAB	<input type="checkbox"/>
Unannounced	<input type="checkbox"/>
Justification	
By _____	
Distribution/	
Availability Codes	
Dist	Avail. for Repro. Special
All	

Approved for public release;
distribution unlimited



	Page
Introduction	1
1. The Ship and Structure	2
2. Propeller Hydrodynamics	6
3. Other Structural and Hydrodynamic Considerations	10
4. Recommendations	13
5. Acknowledgments	14
6. References	15
Appendix A: Nozzle Analysis	16
Appendix B: Propeller Blade Geometry	21
Appendix C: Propeller Forces	37
Appendix D: Structural Analysis of the Blade Under Ice Loading	56

INTRODUCTION

This report presents an evaluation of the proposed kort nozzle for the 140 WYTM Cutter. It considers the shroud structure, the propeller hydrodynamics, the ice loading on the propeller blade, a possible ice deflection strut, and overall design of the kort nozzle. The shroud structure is considered first in Section 1, where it is found to be sufficiently strong. Section 2 goes into the propeller hydrodynamics, while Section 3 considers the remaining topics.

One serious problem with the present design is that there is no access to the propeller. Unless the port, starboard, or both sides of the nozzle is removable, the propeller would have to be installed and the shroud built around it. The screw would be inaccessible for repairs. Suggestions for how this problem could be solved are put forward in Section 1.

The thrust and efficiency of the propeller together with the shroud meet requirements. However, the local velocity distributions are not hydrodynamically the best and result in cavitation on portions of the back and face of the blades. Slight modifications to the sections should alleviate this situation; a very efficient subcavitating propeller should result. Details may be found in Section 2 and Appendix C.

Unless the propeller blades are to be steel, they are not strong enough to withstand extreme ice loading. Details of the ice loading are given in Section 3 and Appendix D. Recommendations 4 and 5 in Section 4 address this problem.

Supports for the nozzle are also discussed in Section 3. These should be faired in to prevent adverse hydrodynamic drag, which reduces the total net thrust.

Recommendations may be found in Section 4.

1. THE SHROUD STRUCTURE

To predict the ice loading to which the nozzle will be subjected is not possible; however, the loading will not exceed the crushing strength of the ice. Graft (1977) suggests using the crushing strength of the ice times the projected area as the upper bound of the compressive force that can be transmitted from the ice to a structure. He also suggests the use of an overall factor of safety ranging from 1.5 to 2.5. Garivick and Lloyd (1970) suggest the use of 300 p.s.i. for the crushing strength of the ice. Since there is no way to anticipate the total area against which the ice will act nor its location, we will use Graft's criterion for the loading. The nozzle will be subjected to 300 p.s.i. acting horizontally as shown in Figure 1-1, since this direction would be the most critical loading. It is assumed that the nozzle will be rigidly supported at the hull; this assumption will be discussed in detail in Section 3.

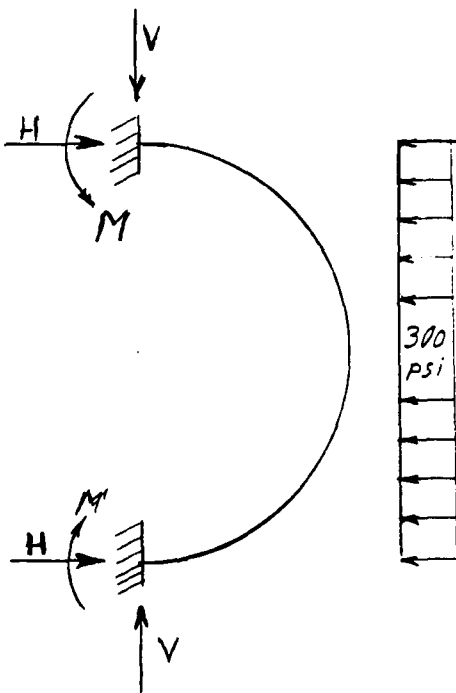


Figure 1-1 NOZZLE LOADING

Each half of the nozzle, the port side and starboard side, will be analyzed as an arch with fixed ends. Figure 1-1 shows both the applied forces and the reaction forces that act on each half. Roark (1954) gives the following expressions for the reactions:

- a) the horizontal reaction H

$$H = WR$$

(1.1)

b) the vertical reaction V

$$V = WR \left(\frac{1}{6} - \frac{1}{4} + \frac{\alpha I}{8} \right)$$
$$\frac{2}{\pi} \left(\frac{I}{2} - 1 \right)^2 - \frac{3I}{4} + 2 - \frac{\alpha I}{4}$$
(1.2)

c) the moment

$$M = \frac{WR^2}{4} - \frac{2HR}{\pi}$$
(1.3)

where R is the radius of the neutral axis, w the loading per linear foot, $\alpha = 1/AR$, and A is the cross sectional area.

Section dimensions and other properties of the shroud are tabulated in Appendix A. The chord c of the nozzle is 4.282 ft; hence, the loading per linear foot is:

$$w = 300 \text{ p.s.i.} * 144 \text{ in}^2 \text{ ft} * 4.282 \text{ ft}$$

$$w = 185,000 \text{ lbs/ft}$$

The neutral axis of the arch is the circle through the centroid of the cross section; its radius R is measured from the center of the propeller shaft and has the value $R = \bar{y} = 4.67$ ft. The section area $A = 2.194 \text{ ft}^2$, and its moment of inertia $I = 0.0961 \text{ ft}^4$.

Substituting these values into equations (1.1) thru (1.3) yields

$$\alpha = \frac{0.961}{2.194 * 4.67} = 0.0020$$

$$H = 185,000 \text{ lbs/ft} * 4.67 \text{ ft}$$

$$= 864,000 \text{ lbs}$$

$$V = 864,000 \text{ lbs} * (-0.0825)/(-0.1503)$$

$$= 474,000 \text{ lbs}$$

$$M = (864,000/4 - 2 * 474,000/11) * 4.67 \text{ ft lb.}$$

$$= - 401,000 \text{ ft lb}$$

The maximum compressive stress σ_{bc} due to bending is given by:

$$\sigma_{bc} = \frac{M}{I} \max (y_u - R)$$
$$= \frac{401,000 \text{ ft lb}}{0.0961 \text{ ft}} (5.34 - 4.67) \text{ ft}$$
$$= 2,796,000 \text{ p.s.f.}$$

$$\sigma_{bc} = 19,400 \text{ p.s.i.}$$

There is an additional compressive stress σ_{ac} due to the axial load H at the support.

$$\begin{aligned}\sigma_{ac} &= H/A \\ &= 864,000 \text{ lbs} / 2.19 \text{ ft}^2 \\ &= 394,000 \text{ p.s.f.} \\ \sigma_{ac} &= 2,740 \text{ p.s.i.}\end{aligned}$$

The maximum compressive stress is:

$$\begin{aligned}\sigma_c &= \sigma_{ac} = \sigma_{hc} \\ &= 2740 \text{ p.s.i.} + 19400 \text{ p.s.i.} \\ \sigma_c &= 22,100 \text{ p.s.i.}\end{aligned}$$

At the fixed support the maximum tensile stress due to bending is

$$\begin{aligned}\sigma_{bt} &= \frac{M}{I} \max (y_1 - R) \\ &= \frac{401,000}{0.0961} (4.67 - 4.37) \text{ p.s.f.} \\ &= 1,251,000 \text{ p.s.f.} \\ \sigma_{bt} &= 8690 \text{ p.s.i.}\end{aligned}$$

Since there is an axial compressive stress, the maximum tensile stress is given by:

$$\begin{aligned}\sigma_t &= \sigma_{bt} - \sigma_{ac} \\ &= 8,690 \text{ p.s.i.} - 2,740 \text{ p.s.i.} \\ \sigma_t &= 5,950 \text{ p.s.i.}\end{aligned}$$

The shear stress τ is given by:

$$\begin{aligned}\tau &= V/A = 474,000 \text{ lbs} / 2.194 \text{ ft}^2 \\ &= 216,000 \text{ p.s.f.} \\ &= 1,500 \text{ p.s.i.}\end{aligned}$$

The internal bending moment around the arch may be expressed as:

$$\begin{aligned}M(\theta) &= -M - VR \sin\theta + HR (1-\cos\theta) - \frac{wR^2}{2} (1-\cos\theta)^2 \\ &= -M - VR \sin\theta + HR (1-\cos\theta) - \frac{HR}{2} (1-\cos\theta)^2\end{aligned}$$

Where M positive indicates inner side (lower surface) in tension.

$$\begin{aligned}M'(\theta) &= -HR \cos\theta + VR \sin\theta - VR(1-\cos\theta) \sin\theta \\&= -HR \cos\theta + VR \cos\theta \sin\theta\end{aligned}$$

The roots of $M'(\theta) = 0$ are $\theta = 0$ and

$$\sin\theta = \frac{HR}{VR} = \frac{H}{V} = \frac{474,000}{864,000} = 0.5486$$

or

$$\theta = 0, 33.27^\circ, \pi - 33.27^\circ$$

The moments at these points have the values

$$M(0) = 205,000 \text{ ft lb}$$

$$M(33.27^\circ) = M(\pi - 33.27^\circ) = -206,000 \text{ ft lb}$$

The level of stress for the arch is small, so that a low carbon steel can be used for its construction. This has the additional advantage that low carbon steels are a tough material with good resistance to impact loading. The nozzle will be subjected to impact loadings from ice at low temperature.

With the present nozzle design there is no access to the propeller. Since the stress level within the shroud is low, the port or both the port and starboard sides could be made removable to provide the necessary access. One approach would be to make the nozzle a built up structure with a cross section like Figure 1.2.

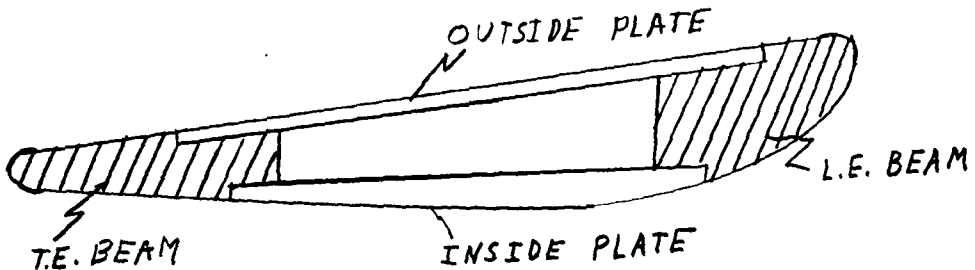


Figure 1.2 BUILT UP SECTION

The structure would consist of a leading edge beam sculptured to the profile of the section and a trailing edge beam also sculptured.

Upper and lower surfaces between the beams would be made from plates. There would be ribs at approximately 45° intervals. The outer and inner surface plates would be made removable. The leading and trailing edge beams would be made removable near the ship hull and the lower support. One approach to these connections would be to have permanent short beams attached to the hull and the lower support; the leading edge and trailing edge beams would bolt to these fixed structures. If this proves impossible, the spacing between the two beams might be made large enough for the prop to fit through. The removable nozzle is however preferable.

2. PROPELLER HYDRODYNAMICS

Fuller (1981b) provided the design criterion for the screw. At a ship speed $V_s = 6$ knots the propeller is to turn at $N = 270$ rpm at a shaft horsepower SHP = 2400 hp. The wake reduction factor is to be $w = 0.177$; this relates to a velocity at $r/R = 0.6$. The axial velocity into the propeller is then given as:

$$V_a = (1-w) V_s = 8.340 \text{ ft/sec}$$

Details of the hydrodynamic force calculations may be found in Appendix C. At the above conditions the thrust developed by the screw is given in Table C-8 as:

$$T = 33,100 \text{ lbs}$$

and the corresponding torque is:

$$\tau = 45,800 \text{ ft lbs.}$$

These values are for a water density $\rho = 1.94 \text{ lbs. sec}^2/\text{ft}$. At this torque the delivered horsepower would be:

$$DHP = \frac{2 \pi n \tau}{550} = 2,354 \text{ Hp}$$

Where $n = 4.5$ r.p.s. is the rotational shaft speed.

$$s = \frac{DHP}{SHP} = 0.981$$

Which is right where it should be.

The thrust coefficient for the screw alone is:

$$K_{Tscrew} = \frac{T}{\rho n^2 D^4} = 0.162,$$

and the torque coefficient is:

$$K_Q = \frac{\tau}{\rho n^2 D^5} = 0.026$$

Van Manen and Superiana (1959) determine the thrust constant of the nozzle

$$K_{Tnozzle} = 0.110;$$

consequently, the total thrust constant is:

$$K_T = K_{Tscrew} + K_{Tnozzle} = 0.272$$

The total thrust is:

$$T = \rho n^2 D^4 K_T = 59,300 \text{ lbs},$$

and the corresponding thrust horsepower THP is:

$$THP = \frac{T V_a}{550} = 899 \text{ Hp}$$

Overall efficiency for the screw nozzle combination is:

$$\eta_0 = \frac{\text{THP}}{\text{DHP}} = 0.382$$

At 258 rpm for a delivered horsepower, DHP = 2350 Hp, the bollard pull due to the propeller is:

$$T_{\text{screw}} = 37,400 \text{ lbs}$$

The thrust coefficient for the screw is:

$$K_{T_{\text{screw}}} = 0.199$$

Adding this to $K_{T_{\text{nozzle}}}$ yields a total thrust coefficient

$$K_T = 0.309$$

for a total thrust

$$T = 58,129 \text{ lbs}$$

This compares with the present bollard pull of 56,000 lbs at 245 rpm. The shroud has reducted the bollard pull of the screw by a third without lowering the total bollard pull.

The velocity distribution is obtained through use of the Goldstein (1952) approximation to Theodoresen's mapping technique. Velocity distributions for $r/R = 0.5, 0.7,$ and 0.9 are shown in Figures 2-1 through 2-3. Details of this method can be found in Appendix C. Although the velocity distribution for the section at $r/R = 0.5$ at a $C_L = 1$, figure 2-4, is quite normal; in contrast, at the design value $C_L = 0.146$ the lower surface velocities exceeds those on the upper surface for the first 15% of the chord. At $r/R = 0.7$ this condition holds over the first 2.5% and at $r/R = 0.9$ over the first 10% but not as drastically as at $r/R = 0.5$. One other bad feature of the velocity distribution is its behavior over the last 25% of the upper surface in the vicinity of $r/R = 0.7$. This erratic behavior is still evident for the same section at $C_L = 1$.

The propeller cavitates under summer operating conditions. Details of the cavitation caluculations are in Appendix C. There is cavitation on the back of the blade at $r/R = 0.7$. There is cavitation along the lower leading edge from an approximate $r/R = 0.5$ to the tip. Both of these conditions are due to poor velocity distribution rather than to an excessive blade loading. It should be possible to operate the propeller cavity free, after minor modifications to the section shape.

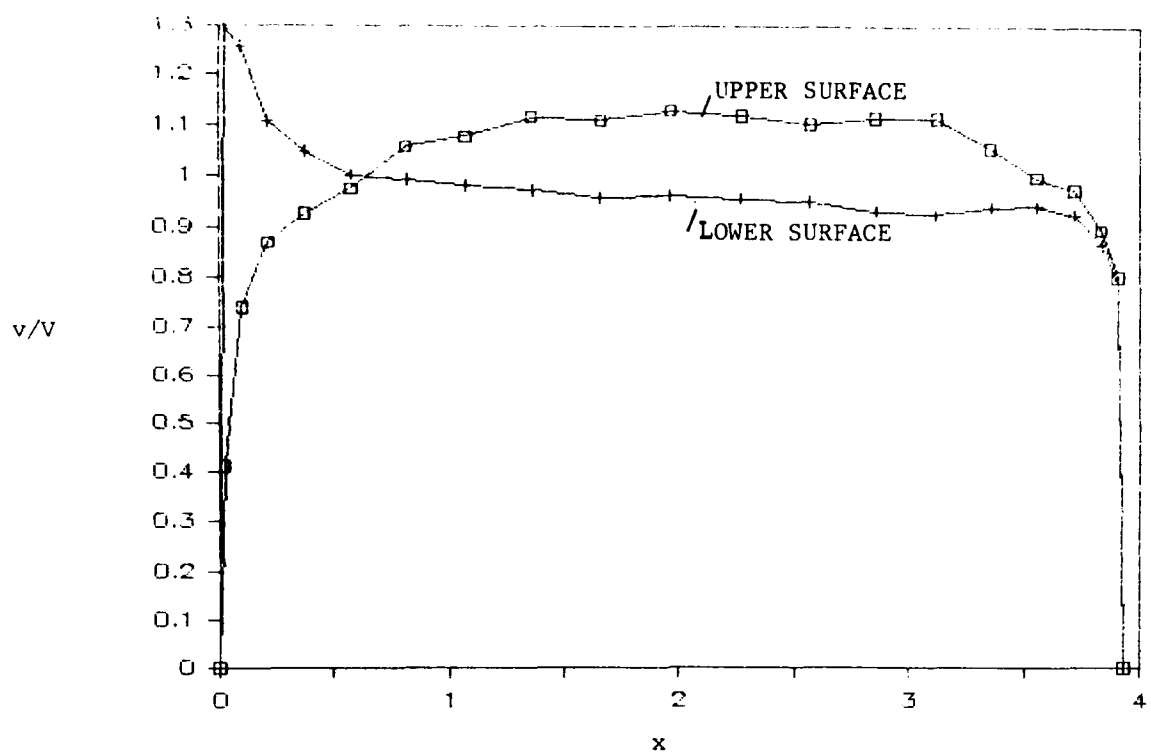


FIGURE 2-1 VELOCITY DISTRIBUTION $r/R=0.5$

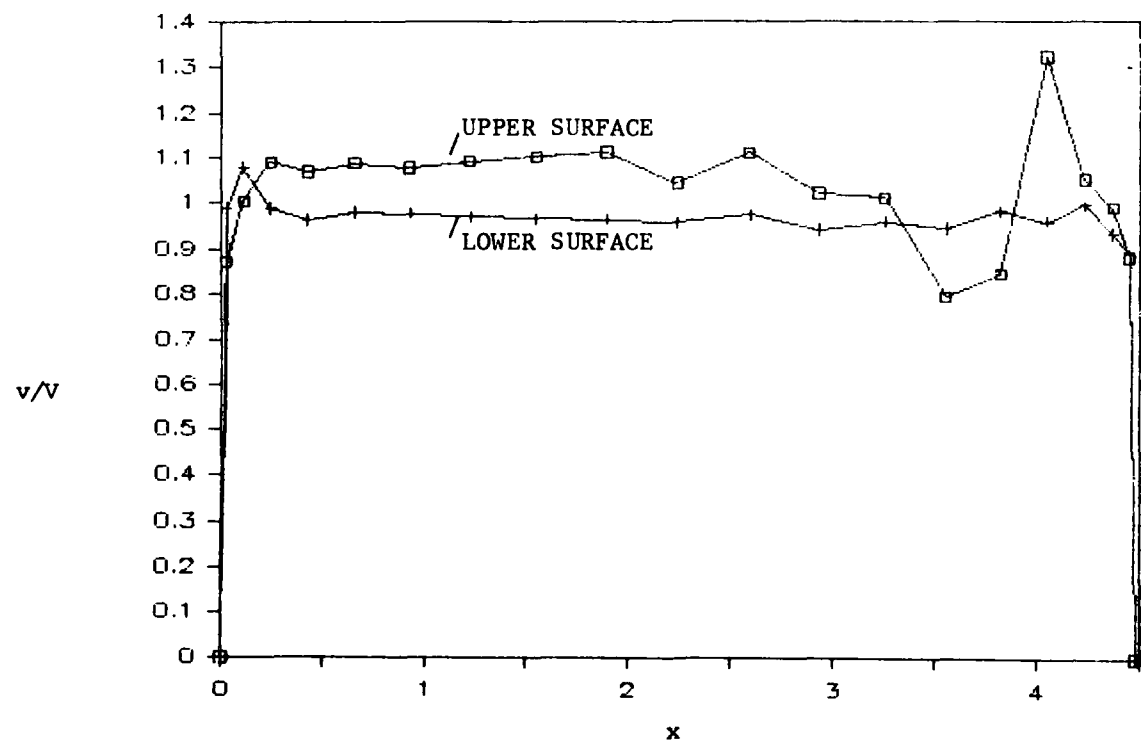


FIGURE 2-2 VELOCITY DISTRIBUTION $r/R=0.7$

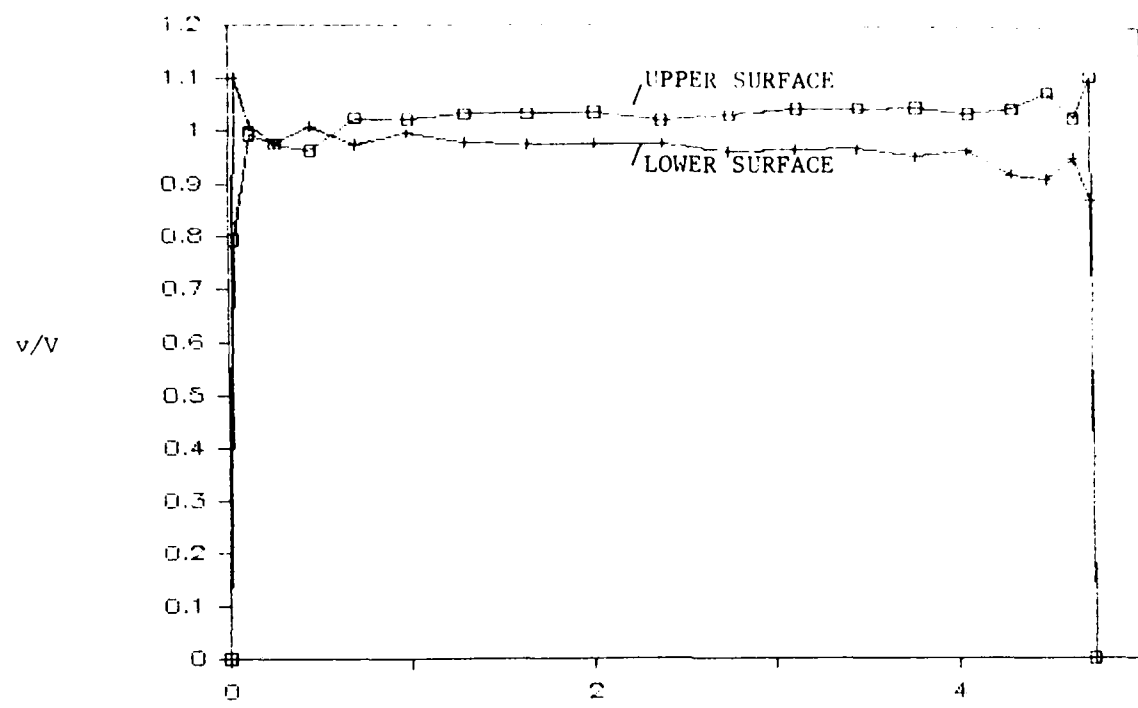


FIGURE 2-3 VELOCITY DISTRIBUTION $r/R=0.9$

3. OTHER STRUCTURAL AND HYDRODYNAMIC CONSIDERATIONS

Stresses due to ice crushing by the blade are tabulated in Table D-6 and were derived in Appendix D. These stresses exceed the design working stresses for both manganese bronze and nickel aluminum bronze screws recommended by O'Brien (1962). In fact the stress levels would actually call for a steel screw. Some might argue that the crushing stress of ice is too severe a loading condition. Consider the results for $r/R = 0.8$; the stress 8800 p.s.i. represents a chunk of ice being forced against the outboard 10.2 inches of the blade. True, the block would have to be 4' wide, but this is plausible. The blade could not support an even smaller block pushing normal to its face; for at $r/R = 0.8$ the appropriate l is 7 in., the maximum distance is 0.039 feet or 0.468 inches, and using an allow stress of 6500 p.s.i., the maximum moment would be

$$M_{\text{allowed}} = \frac{6500 \text{ p.s.i.} * 7 \text{ in}}{0.468 \text{ in}} = 97.222 \text{ in lb}$$

A 10 inch thick by 10 inch wide piece of ice, acting with a 5 inch moment arm, would nearly have to exert 194 p.s.i. to achieve this level of stress.

A strut stretched between the hull and the shroud as shown in Figure 3-1 could be used to deflect ice away from the blades. It would not however protect the blades from ice coming in astern during backing operations. An NACA 0018 section would be sufficiently strong to withstand ice loading, as the predicted maximum stress would be 7780 p.s.i., see Appendix D. It is not possible to predict the direction of flow into the strut; a visual study in a water channel would be advisable to check out the hydrodynamics of the strut and its interaction with the propeller.

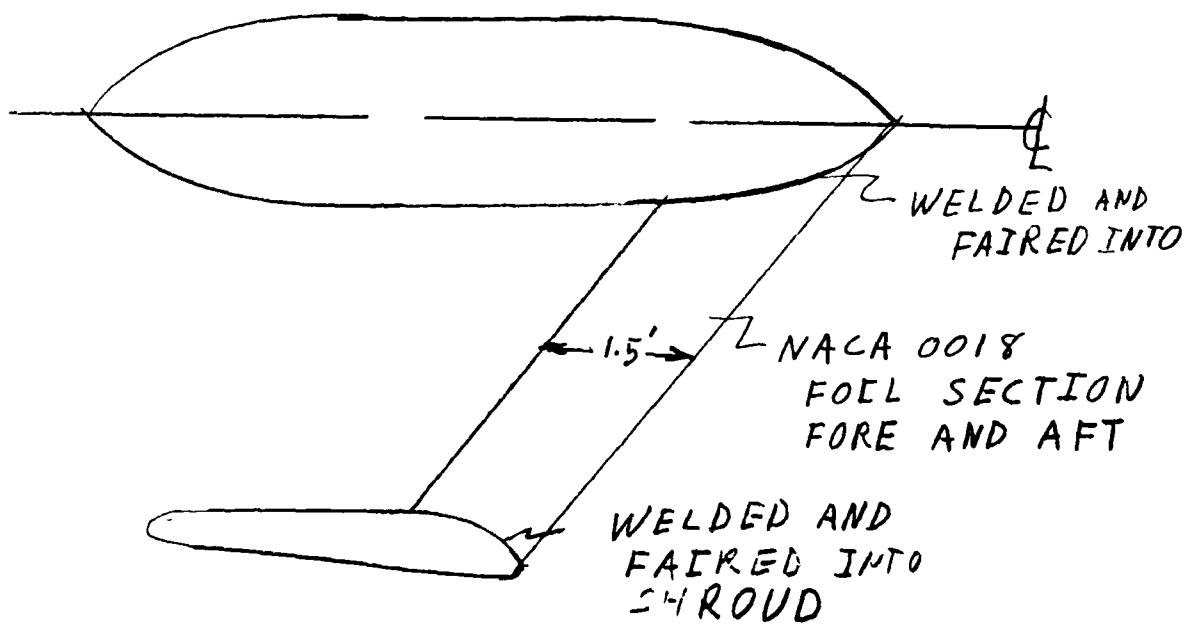


FIGURE 3-1 ICE DEFLECTION STRUT

For hydrodynamic reasons the upper and lower supports for the nozzle should be faired into the ship hull. Structurally they should be made an integral part of the hull, so that they act as rigid supports for the nozzle. Figure 3-2 shows a cut through the upper support (shaded portion) to show the fairing. The width of the support should be determined by the location of its lower outside

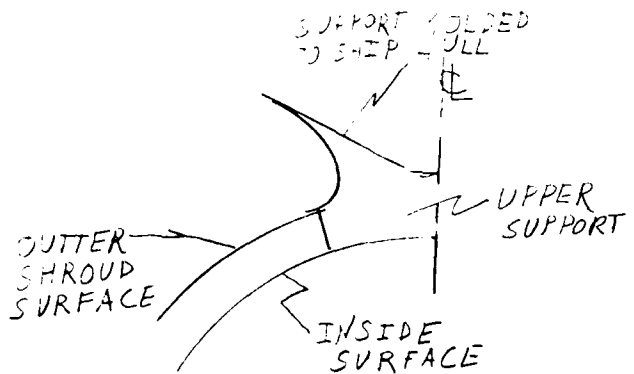


Figure 3-2 ATHWART SHIP CUT THROUGH UPPER SUPPORT

edge; this edge should be located so that it just provides clearance enough to remove the propeller. This is approximately the 1' 6" buttocks plane. Figure 3-3 shows a typical fore and aft section. Two major features are the slots into

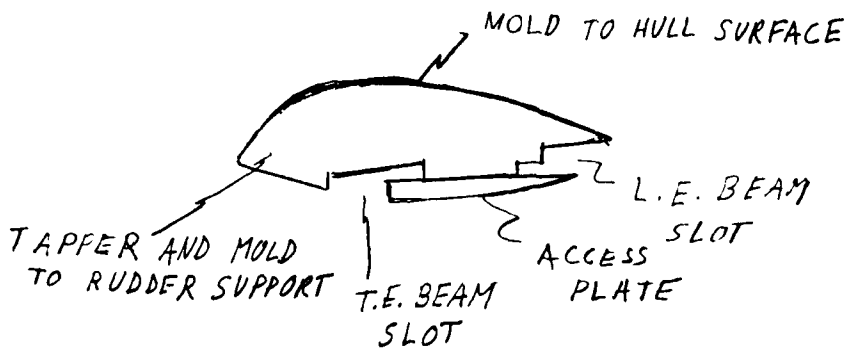


Figure 3-3 FORE AND AFT SECTION

which the shroud leading edge beam and its trailing edge beam fit. These beams should bolt to the support. It may be useful to have an access plate at mid chord to access these bolts; this view shows this plate. Note also that the support continues to the rudder support housing and should be faired into this structure.

Figure 3-4 shows a stern view of a section through the lower support.

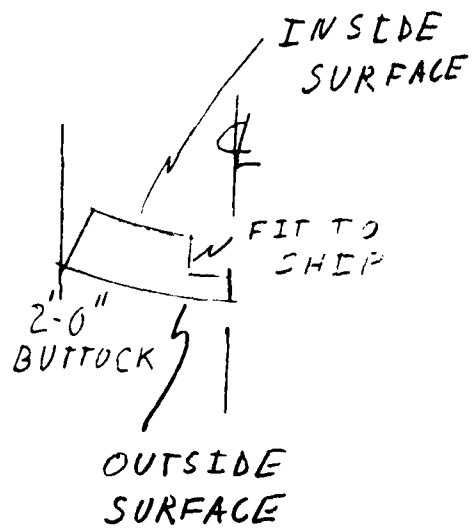


Figure 3-4 LOWER SUPPORT SECTION STERN VIEW

4. RECOMMENDATIONS

1. The nozzle structure should be made removable to provide access to the propeller.
2. Either the pitch angle, the slope of the mean line, or both should be adjusted so the sections operate closer to optional C_L and the unusually high velocities on the face near the leading edge are reduced.
3. Section thickness distributions should be investigated to determine if they cause the cavitation on the back of the blade. Velocity distributions are not properly distributed and the section shape needs modification to alleviate the situation.
4. If the present cutter propellers have not received any significant ice damage, these propellers should be analyzed to determine the maximum stresses they will support at different r/R values for a safety factor of two. These values could then be used as ice load design stresses for the propeller under consideration in this report.
5. Either strengthen the blades to support the loading described in Appendix D or design to the stresses described in recommendation 4.

5. ACKNOWLEDGEMENTS

I would like to thank Professor Rameswar Bhattachayya, Chairman of the Naval Systems Engineering Department of the United States Naval Academy for introducing me to the Burril method and for many hours of technical discussion pertinent to this paper. I would also like to thank Commander Neil J. Collins, Executive Assistant of the same department, for his assistance in expediting the publication of this report and for enduring the many other administrative headaches that went with its publication.

6. REFERENCES

- Abbott, Ira H. and Albert E von Doenhoff (1949), Theory of Wing Sections, Dover Publications, Inc., New York.
- Burriel, L. C. (1944), Calculation of marine propeller performance characteristics, Transactions N.E.C.I. 195.
- Fuller, Nathan R. Jr. (1981a), United States Coast Guard Drawing, Kort Nozzle for 140 WYTM Cutter.
- Fuller, Nathan R. Jr. (1981b), Design notes.
- Goldstein, S. (1952), Approximate two-dimensional airfoil theory. Parts I-VI, Curr. Pap Aero. Res. Coun. London 128, 140, 141.
- Graft, William (1977), Mechanical Properties of sea ice as they influence design considerations, Interpipe 77, The fifth International Pipeline Technology Convention, Houston, Texas.
- Langan, Thomas J. and Henry T. Wang (1974), Evaluation of lifting - surface programs for computing the pressure distribution on planar wings in steady motion, Computers and Fluids 2, 53-78.
- O'Brien, T. P. (1962), The Design of Marine Screw Propellers, Hutchinson Scientific and Technical, London.
- Roark, Raymond J. (1954), Formulas for Stress and Strain, McGraw Hill Book Company, Inc..
- Thwaites, Bryan (1960), Incompressible Aerodynamics, Oxford at the Clarendon Press, Oxford, England.
- Van Manen, J. D. and A. Superian (1959), The design of screw-propellers in nozzles, International Shipbuilding Progress 6, 95-113.

APPENDIX A NOZZLE ANALYSIS

The shroud dimensions in this report are from the 140 WYTM Cutter Propeller Data which are stored on the Naval Academy Time Sharing System (NATS). This data was digitized from the United States Coast Guard Drawing (Fuller 1981a). The section data presented in Table A-1 is good to 0.005 ft, i.e. ± 0.06 inches. Both y_u and y_l are scaled data; whereas, the fore and aft coordinate X is a direct reading in inches from the drawing. x is the scaled version of X , where the scale factor $1'/1.5"$ is used.

TABLE A-1 SHROUD SECTION

Upper Surface			Lower Surface		
<u>X</u> (in)	x (ft)	y_u (ft)	<u>X</u> (in)	x (ft)	y_l (ft)
3.176	2.117	5.114	3.176	2.117	5.114
3.125	2.083	5.180	3.038	2.025	4.906
3.025	2.017	5.233	2.621	1.747	4.650
2.925	1.530	5.240	2.183	1.455	4.481
2.236	1.491	5.150	1.584	1.056	4.371
-0.022	-0.015	4.918	0.774	0.516	4.314
-0.022	-0.015	4.925	-0.106	-0.070	4.316
-0.092	-0.061	4.898	-1.536	-1.024	4.330
-1.790	-1.193	4.730	-2.586	-1.724	4.372
-3.118	-2.125	4.590	-3.106	-2.701	4.402
-3.228	-2.152	4.549	-3.207	-2.138	4.436
-3.247	-2.165	4.482	-3.247	-2.165	4.482

TABLE A-2 presents this section data as a function of the nondimensional distance

$$x^1 = (x_{LE} - x)/c$$

where x_{LE} is the x-coordinate of the leading edge. From the table $x_{LE} = 2.117$ ft; c is the section chord length and is given as

$$c = x_{LE} - x_{TE}$$

T.E. denotes trailing edge; from the table $x_{TE} = -2.165$ ft. Hence,

$$c = 2.117 - (-2.165) = 4.282 \text{ ft.}$$

In the table n.t. denotes nose to tail line, i.e. the line between the leading edge and the trailing edge. Y_C is the camber line approximation:

$$Y_C = 0.5 (Y_u + Y_l) - n.t.$$

The upper surface coordinate Y_u and lower surface coordinate Y_l are linear interpolations of the data in Table A-1. The maximum thickness of the shroud is 0.712 ft from the tabulated values of $Y_u - Y_l$, and this minimum thickness occurs at 25% of the chord. Maximum camber also occurs at 25% of the chord and has the absolute value 0.230 ft.

TABLE A-2 SECTION DIMENSIONS FOR SHPNUUD

x'	x(ft)	y_u(ft)	y_1(ft)	y_u-y_1 (ft)	0.5+(y_u+y_1)t (ft)	n.t.	y_c(ft)
0.000	2.117	5.114	5.114	0.000	5.114	5.114	0.000
0.0125	2.064	5.195	4.993	0.202	5.094	5.106	-0.012
0.025	2.010	5.234	4.889	0.345	5.062	5.098	-0.037
0.050	1.903	5.231	4.774	0.457	5.003	5.082	-0.080
0.075	1.796	5.210	4.658	0.552	4.943	5.067	-0.133
0.100	1.689	5.189	4.580	0.609	4.885	5.051	-0.166
0.15	1.475	5.148	4.489	0.659	4.819	5.019	-0.201
0.20	1.261	5.115	4.427	0.688	4.771	4.988	-0.217
0.25	1.047	5.082	4.370	0.712	4.726	4.956	-0.230
0.30	0.833	5.048	4.347	0.701	4.698	4.924	-0.227
0.35	0.619	5.016	4.325	0.691	4.671	4.893	-0.222
0.40	0.405	4.983	4.314	0.669	4.649	4.861	-0.213
0.45	0.190	4.950	4.315	0.635	4.633	4.830	-0.197
0.50	-0.024	4.914	4.316	0.598	4.615	4.798	-0.183
0.55	-0.238	4.872	4.318	0.554	4.595	4.766	-0.171
0.60	-0.452	4.840	4.322	0.518	4.581	4.735	-0.154
0.65	-0.666	4.808	4.325	0.483	4.567	4.703	-0.137
0.70	-0.880	4.776	4.325	0.448	4.552	4.672	-0.120
0.75	-1.084	4.745	4.334	0.411	4.540	4.640	-0.101
0.80	-1.308	4.712	4.347	0.365	4.530	4.608	-0.079
0.85	-1.522	4.677	4.360	0.317	4.519	4.577	-0.058
0.90	-1.736	4.644	4.373	0.307	4.491	4.545	-0.055
0.95	-1.951	4.609	4.392	0.217	4.501	4.514	-0.013
1.00	-2.165	4.482	4.482	0	4.482	4.482	0.000

Section properties for the shroud are calculated by dividing the shroud section into elements $\Delta x = 0.05$ units wide, as shown in Figure A-1.

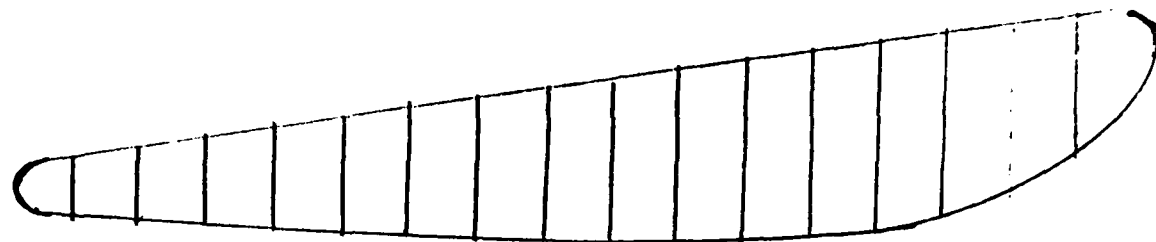


Figure A-1 DIVISION OF SHROUD

Since $y_u - y_l = 0$ at both the leading and trailing edges, the section's total area A in terms of the trapazoidal rule is:

$$A = 0.05c \sum (y_u - y_l)$$

By definition and the trapazoidal rule the location \bar{y} of the section centroid from the axis of the propeller shaft is:

$$\bar{y} = 0.05c \sum \bar{y}_i (y_u - y_l)_i / A,$$

where $\bar{y}_i = (y_u + y_l)/2$. Since the centroid of each element is not located at the same distance from the propeller axis as the centroid of the section but is additional $\bar{y}_i - \bar{y}$ away, it is useful to use the parallel axis theorem. When this is done, the moment of inertia I around the centroidal axis for the shroud section is given by:

$$I = 0.05c (\sum (y_u - y_l)(\bar{y}_i - \bar{y})^2 + \sum I_i)$$

where $I_i = (y_u - y_l)^3 / 12$.

TABLE A-3 SECTION PROPERTIES

x'	$y_u - y_1$ (ft)	\bar{y}_1 (ft)	$\bar{y}_1^* (y_u - y_1) (\text{ft})^2$	$\bar{y}_1 - \bar{y}$ (ft)	$(y_u - y_1)(\bar{y}_1 - \bar{y}) \text{ft}^2$	$(y_u - y_1)(\bar{y}_1 - \bar{y})^2 (\text{ft})^3$	$\bar{I}_1 (\text{ft}^3)$
0.000	0.000	5.114	0.000	0.444	0.000	0.0000	0.0000
0.05	0.457	5.003	2.286	0.332	0.152	0.0504	0.0080
0.10	0.609	4.885	2.975	0.214	0.130	0.0279	0.0188
0.15	0.659	4.819	3.175	0.148	0.098	0.0145	0.0238
0.20	0.688	4.771	3.282	0.101	0.069	0.0070	0.0271
0.25	0.712	4.726	3.365	0.056	0.040	0.0022	0.0301
0.30	0.701	4.698	3.293	0.027	0.019	0.0005	0.0287
0.35	0.691	4.671	3.227	0.000	0.000	0.0000	0.0275
0.40	0.669	4.649	3.110	-0.022	-0.015	0.0003	0.0250
0.45	0.635	4.633	2.924	-0.038	-0.024	0.0009	0.0213
0.50	0.598	4.615	2.760	-0.055	-0.033	0.0018	0.0178
0.55	0.554	4.595	2.546	-0.075	-0.042	0.0031	0.0142
0.60	0.518	4.581	2.373	-0.089	-0.046	0.0041	0.0116
0.65	0.483	4.567	2.206	-0.104	-0.050	0.0052	0.0094
0.70	0.448	4.552	2.039	-0.118	-0.053	0.0063	0.0075
0.75	0.411	4.540	1.866	-0.131	-0.054	0.0070	0.0058
0.80	0.365	4.530	1.653	-0.141	-0.051	0.0070	0.0041
0.85	0.317	4.519	1.432	-0.152	-0.048	0.0073	0.0027
0.90	0.307	4.491	1.379	-0.180	-0.055	0.0099	0.0024
0.95	0.217	4.501	0.977	-0.170	-0.037	0.0063	0.0009
1.00	0.000	4.482	0.000	-0.188	0.000	0.0000	0.0000
Σ	10.039	-----	46.885	-----	0.000	0.1621	0.2865

$$A = 2.194 \text{ ft}^2$$

$$\bar{y} = 4.670 \text{ ft}$$

$$I = 0.0961 \text{ ft}^4 = 1992 \text{ in}^4$$

APPENDIX R: PROPELLER BLADE GEOMETRY

The propeller dimensions presented in this report are obtained from the 140 WYTM Cutter K 3-75 Propeller Data stored on NATS. This data was digitized from United States Coast Guard Drawing (Fuller 1981a). The section data presented in Tables B1 through B7 is good to ± 0.005 ft. which is the same as ± 0.06 in. The propeller radius $R = 4.25$ ft.

TABLE B1 DIGITIZED SECTION DATA $r/R = 0.4$

Upper Surface		Lower Surface	
x (ft)	y_u (ft)	x (ft)	y_l (ft)
1.851	0.198	1.851	0.198
1.850	0.214	1.835	0.180
1.835	0.226	1.769	0.182
1.768	0.256	1.597	0.176
1.656	0.304	1.426	0.177
1.481	0.359	1.297	0.174
1.323	0.404	1.108	0.166
1.113	0.450	0.859	0.166
0.851	0.499	0.622	0.170
0.633	0.519	0.386	0.168
0.393	0.529	0.152	0.170
0.187	0.532	-0.005	0.173
0.001	0.534	-0.269	0.165
-0.002	0.532	-0.566	0.175
-0.049	0.527	-0.860	0.170
-0.238	0.516	-0.991	0.171
-0.421	0.501	-1.132	0.174
-0.744	0.464	-1.334	0.183
-0.965	0.418	-1.514	0.187
-1.783	0.345	-1.689	0.194
-1.482	0.290	-1.750	0.196
-1.603	0.259	-1.753	0.200
-1.726	0.220	-1.756	0.204
-1.754	0.210		
-1.756	0.204		

TABLE B-2 DIGITIZED SECTION DATA $r/R = 0.5$

Upper Surface		Lower Surface	
x (ft)	y_u (ft)	x (ft)	y_l (ft)
1.988	0.193	1.988	0.193
1.982	0.199	1.984	0.175
1.972	0.209	1.966	0.167
1.913	0.223	1.932	0.165
1.788	0.258	1.831	0.162
1.621	0.295	1.686	0.161
1.441	0.332	1.448	0.165
1.196	0.381	1.248	0.165
0.892	0.424	1.047	0.166
0.631	0.449	0.686	0.165
0.393	0.461	0.162	0.169
0.299	0.464	0.001	0.167
-0.004	0.468	-1.181	0.170
-0.082	0.467	-0.408	0.166
-0.318	0.457	-0.638	0.172
-0.522	0.443	-0.911	0.176
-0.739	0.430	-1.207	0.174
-1.027	0.397	-1.396	0.172
-1.225	0.369	-1.618	0.172
-1.434	0.319	-1.810	0.181
-1.702	0.260	-1.935	0.182
-1.838	0.223	-1.941	0.182
-1.915	0.206		
-1.937	0.196		
-1.941			

TABLE B-3 DIGITIZED SECTION DATA $r/R = 0.6$

Upper Surface		Lower Surface	
x (ft)	y_u (ft)	x (ft)	y_l (ft)
1.990	0.191	1.990	0.191
1.980	0.205	1.978	0.175
1.946	0.217	1.938	0.165
1.823	0.246	1.852	0.160
1.701	0.266	1.722	0.161
1.556	0.289	1.485	0.159
1.217	0.328	1.265	0.161
0.688	0.378	0.956	0.167
0.372	0.396	0.612	0.166
0.001	0.403	0.222	0.165
0.001	0.399	-0.001	0.167
-0.134	0.402	-0.241	0.167
-0.416	0.392	-0.620	0.172
-0.616	0.386	-0.983	0.172
-0.807	0.370	-1.322	0.173
-1.037	0.354	-1.630	0.172
-1.315	0.322	-1.892	0.170
-1.490	0.300	-2.052	0.171
-1.712	0.266	-2.098	0.173
-1.855	0.245	-2.108	0.180
-2.002	0.214		
-2.072	0.201		
-2.100	0.193		
-2.108	0.180		

TABLE B- 4 DIGITIZED SECTION DATA r/R = 0.7

Upper Surface		Lower Surface	
x (ft)	Y _u (ft)	x (ft)	Y _l (ft)
2.242	0.181	2.242	0.181
2.238	0.191	2.240	0.169
2.196	0.195	2.228	0.163
1.982	0.222	2.150	0.162
1.766	0.242	2.023	0.163
1.494	0.274	1.872	0.166
0.971	0.314	1.678	0.163
0.467	0.330	1.404	0.164
0.001	0.333	1.158	0.166
-0.001	0.334	0.640	0.168
-0.404	0.331	0.309	0.170
-0.680	0.325	0.116	0.168
-0.952	0.315	-0.092	0.173
-1.174	0.301	-0.382	0.170
-1.478	0.276	-0.707	0.178
-1.659	0.261	-0.989	0.175
-1.804	0.248	-1.326	0.175
-2.052	0.215	-1.570	0.171
-2.167	0.202	-1.850	0.173
-2.227	0.192	-2.046	0.171
-2.233	0.184	-2.179	0.174
		-2.227	0.178
		-2.233	0.184

TABLE B-5 DIGITIZED SECTION DATA $r/R = 0.8$

Upper Surface		Lower Surface	
x (ft)	y _u (ft)	x (ft)	y _l (ft)
2.321	0.178	2.321	0.178
2.315	0.188	2.309	0.164
2.277	0.190	2.243	0.159
2.162	0.201	2.168	0.163
2.018	0.208	2.037	0.162
1.920	0.215	1.880	0.164
1.706	0.227	1.680	0.165
1.399	0.243	1.452	0.165
0.937	0.266	1.192	0.169
0.508	0.282	0.745	0.169
0.002	0.284	0.480	0.169
-0.002	0.286	-0.003	0.171
-0.069	0.282	-0.320	0.167
-0.282	0.282	-0.691	0.178
-0.603	0.279	-1.090	0.179
-1.002	0.272	-1.368	0.172
-1.395	0.253	-1.576	0.173
-1.568	0.241	-1.931	0.170
-1.756	0.232	-2.122	0.172
-1.925	0.220	-2.282	0.175
-2.256	0.198	-2.322	0.175
-2.314	0.191	-3.324	0.181
-2.324	0.181		

TABLE B-6 DIGITIZED SECTION DATA $r/R = 0.9$

Upper Surface		Lower Surface	
x (ft)	y_u (ft)	x (ft)	y_l (ft)
2.373	0.168	2.373	0.168
2.372	0.172	2.372	0.164
2.355	0.180	2.315	0.164
2.287	0.186	2.134	0.162
2.168	0.195	1.938	0.165
2.065	0.194	1.638	0.164
1.910	0.201	1.359	0.168
1.736	0.214	0.815	0.166
1.536	0.222	0.329	0.170
1.190	0.233	-0.003	0.171
0.756	0.240	-0.396	0.170
0.407	0.241	-1.161	0.174
0.004	0.244	-1.886	0.176
-0.002	0.238	-2.193	0.174
-0.570	0.243	-2.308	0.175
-1.312	0.235	-2.368	0.172
-1.637	0.223	-2.374	0.180
-1.830	0.219		
-2.163	0.198		
-2.296	0.193		
-2.372	0.186		
-2.374	0.180		

TABLE R-7 DIGITIZED SECTION DATA $r/R = 1.0$

Upper Surface		Lower Surface	
x (ft)	Y_u (ft)	x (ft)	Y_l (ft)
2.388	0.172	2.388	0.172
2.382	0.178	2.386	0.160
2.353	0.182	2.376	0.160
2.228	0.191	2.337	0.166
2.061	0.196	2.259	0.161
1.918	0.199	2.166	0.167
1.526	0.214	2.035	0.164
1.202	0.217	1.829	0.164
0.682	0.223	1.287	0.164
-0.002	0.224	0.786	0.168
-0.002	0.227	0.208	0.169
-0.129	0.229	0.001	0.169
-0.373	0.223	-0.511	0.171
-0.588	0.227	-1.074	0.177
-0.826	0.227	-1.524	0.173
-1.177	0.220	-2.007	0.177
-1.586	0.213	-2.177	0.174
-1.826	0.203	-2.300	0.171
-1.979	0.202	-2.376	0.170
-2.163	0.194	-2.380	0.178
-2.300	0.193		
-2.374	0.186		
-2.380	0.178		

The expanded blade data, presented in Table B-8, was derived from Tables B-1 through B-7. The leading edge L, E. is the largest positive value of X, and the trailing edge T, E. is the largest negative value. Camber c is the distance between the leading and trailing edges. Maximum thickness for this propeller blade is at X = 0; the value in the table is computed using the maximum value of Y_u and the value of Y_l nearest X = 0. All values for $r/R = 0.3$ were taken from the drawing by Fuller (1981a).

TARLF R-8 EXPANDED BLADE GEOMETRY

R = 4.25 ft					
r/R	r(ft)	L.E. (ft)	T. E. (ft)	c (ft)	t (ft)
0.3	1.275	1.68	-1.52	3.20	0.424
0.4	1.700	1.851	-1.756	3.607	0.361
0.5	2.125	1.988	-1.941	3.929	0.301
0.6	2.550	1.990	-2.108	4.098	0.236
0.7	2.975	2.242	-2.233	4.475	0.161
0.8	3.400	2.321	-2.324	4.645	0.115
0.9	3.825	2.373	-3.374	4.474	0.073
1.0	4.250	2.388	-2.380	4.768	0.055

It is convenient to have all section data as a function of the nondimensional distance

$$x' = \frac{x_{LE} - x}{c}$$

from the leading edge for the purpose of computing the pressure on each wing section. This data is tabulated in Tables B-10 thru B-15. In the tables n.t. denotes the nose to tail line or chord line; it is the line between the leading edge and the trailing edge. y_c is the camber line approximation

$$y_c = 0.5 (y_u + y_l) - n.t.$$

The upper surface coordinate y_u and the lower surface coordinate y_l are linear interpolations of the respective data in Tables B-1 through B-7.

TABLE B-9 SECTION DIMENSIONS AS FUNCTIONS OF NON DIMENSIONAL DISTANCE FROM L.E. $r/R = 0.4$

x'	$x(\text{ft})$	$y_d(\text{ft})$	$y_l(\text{ft})$	$y_u-y_l(\text{ft})$	$(y_u+y_l)/2(\text{ft})$	n.t.	$y_c(\text{ft})$
0.000	1.851	0.198	0.198	0.000	0.198	0.198	0.000
0.0125	1.806	0.239	0.181	0.058	0.210	0.198	0.012
0.025	1.761	0.259	0.182	0.077	0.220	0.198	0.022
0.050	1.671	0.298	0.179	0.119	0.238	0.198	0.040
0.075	1.580	0.328	0.176	0.152	0.252	0.198	0.054
0.100	1.490	0.356	0.177	0.179	0.266	0.199	0.067
0.15	1.310	0.407	0.174	0.233	0.290	0.199	0.091
0.20	1.130	0.446	0.167	0.279	0.310	0.199	0.111
0.25	0.949	0.481	0.166	0.315	0.324	0.200	0.124
0.30	0.769	0.506	0.168	0.338	0.337	0.200	0.137
0.35	0.589	0.521	0.170	0.351	0.346	0.200	0.146
0.40	0.408	0.528	0.168	0.360	0.348	0.200	0.148
0.45	0.228	0.531	0.169	0.362	0.350	0.201	0.149
0.50	0.048	0.534	0.172	0.362	0.353	0.201	0.152
0.55	-0.133	0.522	0.169	0.353	0.346	0.201	0.145
0.60	-0.313	0.510	0.166	0.344	0.338	0.202	0.136
0.65	-0.494	0.493	0.172	0.321	0.332	0.202	0.130
0.70	-0.674	0.472	0.173	0.299	0.322	0.202	0.120
0.75	-0.854	0.441	0.170	0.271	0.306	0.202	0.104
0.80	-1.035	0.402	0.171	0.253	0.286	0.203	0.083
0.85	-1.215	0.361	0.178	0.183	0.270	0.203	0.067
0.90	-1.395	0.314	0.184	0.130	0.249	0.203	0.046
0.95	-1.576	0.266	0.190	0.076	0.228	0.204	0.024
1.00	-1.756	0.204	0.204	0.000	0.204	0.204	0.000

TABLE R-10 SECTION DIMENSIONS AS FUNCTIONS OF NON DIMENSIONAL DISTANCE FROM L.F. $r/R = 0.5$

x'	x (ft)	y_u (ft)	y_l (ft)	$y_u - y_l$ (ft)	$(y_u + y_l)/2$ (ft)	n.t.	y_c (ft)
0.000	1.988	0.193	0.193	0.000	0.193	0.193	0.0000
0.0125	1.939	0.217	0.165	0.052	0.191	0.193	-0.002
0.025	1.89	0.229	0.164	0.065	0.196	0.193	0.003
0.050	1.792	0.257	0.162	0.095	0.210	0.193	0.017
0.075	1.693	0.279	0.161	0.118	0.220	0.193	0.027
0.100	1.595	0.300	0.162	0.138	0.231	0.193	0.038
0.15	1.399	0.340	0.165	0.175	0.252	0.193	0.060
0.20	1.202	0.380	0.165	0.215	0.272	0.193	0.080
0.25	1.006	0.408	0.166	0.242	0.287	0.193	0.094
0.30	0.809	0.432	0.165	0.267	0.298	0.193	0.106
0.35	0.613	0.450	0.166	0.284	0.308	0.193	0.115
0.40	0.416	0.460	0.167	0.293	0.314	0.193	0.120
0.45	0.220	0.464	0.169	0.295	0.316	0.193	0.124
0.50	0.024	0.468	0.167	0.301	0.318	0.193	0.126
0.55	-0.173	0.463	0.169	0.294	0.316	0.192	0.124
0.60	-0.369	0.454	0.168	0.286	0.312	0.192	0.120
0.65	-0.566	0.440	0.170	0.270	0.305	0.192	0.113
0.70	-0.762	0.427	0.171	0.256	0.299	0.192	0.107
0.75	-0.959	0.405	0.176	0.229	0.290	0.192	0.098
0.80	-1.155	0.379	0.174	0.205	0.276	0.192	0.084
0.85	-1.352	0.339	0.172	0.157	0.256	0.192	0.064
0.90	-1.548	0.294	0.172	0.122	0.233	0.192	0.041
0.95	-1.745	0.248	0.178	0.071	0.213	0.192	0.027
1.00	-1.941	0.192	0.192	0.000	0.192	0.192	0.000

TABLE R-11 SECTION DIMENSIONS AS FUNCTIONS OF NON DIMENSIONAL DISTANCE FROM L.E. $r/R = 0.6$

x'	$x(\text{ft})$	$y_u(\text{ft})$	$y_l(\text{ft})$	$y_u - y_l (\text{ft})$	$(y_u + y_l)/2 (\text{ft})$	n.t.	$y_c(\text{ft})$
0.000	1.990	0.191	0.191	0.000	0.191	0.191	0.000
0.0125	1.939	0.219	0.165	0.054	0.192	0.191	0.001
0.025	1.888	0.231	0.162	0.069	0.196	0.191	0.005
0.050	1.785	0.252	0.160	0.092	0.206	0.190	0.016
0.075	1.683	0.269	0.161	0.108	0.215	0.190	0.025
0.100	1.580	0.285	0.160	0.125	0.222	0.190	0.032
0.15	1.375	0.310	0.160	0.150	0.235	0.190	0.045
0.20	1.170	0.332	0.163	0.169	0.248	0.189	0.059
0.25	0.966	0.352	0.167	0.185	0.260	0.189	0.071
0.30	0.761	0.371	0.166	0.205	0.268	0.188	0.080
0.35	0.556	0.386	0.166	0.220	0.276	0.187	0.089
0.40	0.351	0.396	0.165	0.231	0.281	0.187	0.094
0.45	0.146	0.400	0.166	0.234	0.283	0.186	0.097
0.50	-0.059	0.403	0.167	0.236	0.285	0.186	0.099
0.55	-0.264	0.397	0.167	0.230	0.282	0.185	0.097
0.60	-0.469	0.391	0.170	0.221	0.280	0.184	0.096
0.65	-0.674	0.381	0.172	0.209	0.276	0.184	0.092
0.70	-0.879	0.365	0.172	0.193	0.268	0.183	0.085
0.75	-1.084	0.349	0.172	0.177	0.260	0.183	0.077
0.80	-1.288	0.325	0.173	0.152	0.249	0.182	0.067
0.85	-1.493	0.300	0.172	0.128	0.236	0.182	0.054
0.90	-1.698	0.270	0.172	0.098	0.221	0.181	0.021
0.95	-1.903	0.235	0.170	0.065	0.203	0.181	0.021
1.00	-2.108	0.180	0.180	0.000	0.180	0.180	0.000

TABLE B-12 SECTION DIMENSIONS AS FUNCTIONS OF NON DIMENSIONAL DISTANCE FROM L.F. $r/R = 0.7$

x'	x (ft)	y_u (ft)	y_l (ft)	$y_u - y_l$ (ft)	$(y_u + y_l)/2$ (ft)	n.t.	y_c (ft)
0.000	2.242	0.181	0.181	0.000	0.181	0.181	0.000
0.0125	2.186	0.196	0.162	0.034	0.179	0.181	0.003
0.025	2.130	0.203	0.162	0.041	0.182	0.181	0.01
0.050	2.018	0.218	0.163	0.055	0.190	0.181	0.009
0.075	1.906	0.229	0.165	0.064	0.197	0.181	0.016
0.100	1.794	0.239	0.165	0.074	0.202	0.181	0.021
0.15	1.571	0.265	0.163	0.102	0.214	0.182	0.032
0.20	1.347	0.283	0.164	0.121	0.224	0.182	0.042
0.25	1.123	0.302	0.166	0.136	0.234	0.182	0.052
0.30	0.900	0.316	0.167	0.149	0.242	0.182	0.060
0.35	0.676	0.323	0.168	0.155	0.246	0.182	0.064
0.40	0.452	0.330	0.169	0.161	0.250	0.182	0.068
0.45	0.228	0.332	0.169	0.163	0.250	0.182	0.068
0.50	0.004	0.333	0.171	0.162	0.252	0.182	0.070
0.55	-0.219	0.332	0.172	0.160	0.252	0.183	0.069
0.60	-0.443	0.330	0.172	0.158	0.251	0.183	0.068
0.65	-0.667	0.326	0.177	0.149	0.252	0.183	0.069
0.70	-0.890	0.317	0.176	0.141	0.246	0.183	0.063
0.75	-1.114	0.305	0.175	0.130	0.240	0.183	0.057
0.80	-1.338	0.283	0.175	0.108	0.220	0.183	0.046
0.85	-1.562	0.269	0.171	0.098	0.220	0.184	0.036
0.90	-1.786	0.250	0.172	0.078	0.211	0.184	0.027
0.95	-2.009	0.221	0.172	0.049	0.196	0.184	0.012
1.00	-2.233	0.184	0.184	0.000	0.184	0.184	0.000

TABLE B-13 SECTION DIMENSIONS AS FUNCTIONS OF NON DIMENSIONAL DISTANCE FROM L.E. $r/R = 0.8$

x'	x (ft)	y_u (ft)	y_l (ft)	$y_u - y_l$ (ft)	$(y_u + y_l)/2$ (ft)	n.t.	y_c (ft)
0.000	2.321	0.178	0.178	0.000	0.178	0.178	0.000
0.0125	2.263	0.196	0.160	0.036	0.178	0.178	0.000
0.025	2.205	0.199	0.161	0.038	0.180	0.178	0.002
0.050	2.089	0.204	0.162	0.042	0.183	0.178	0.005
0.075	1.973	0.211	0.163	0.048	0.187	0.178	0.009
0.100	1.856	0.219	0.164	0.055	0.192	0.178	0.014
0.15	1.624	0.231	0.165	0.066	0.198	0.178	0.020
0.20	1.392	0.243	0.167	0.076	0.205	0.179	0.026
0.25	1.160	0.254	0.169	0.085	0.212	0.179	0.033
0.30	0.928	0.266	0.169	0.097	0.218	0.179	0.039
0.35	0.695	0.275	0.169	0.106	0.222	0.179	0.043
0.40	0.463	0.282	0.169	0.113	0.226	0.179	0.047
0.45	0.231	0.283	0.170	0.113	0.226	0.179	0.047
0.50	-0.002	0.286	0.171	0.115	0.228	0.179	0.049
0.55	-0.234	0.282	0.168	0.114	0.225	0.179	0.046
0.60	-0.466	0.280	0.171	0.109	0.226	0.180	0.046
0.65	-0.698	0.277	0.178	0.099	0.228	0.180	0.048
0.70	-0.930	0.273	0.179	0.094	0.226	0.180	0.046
0.75	-1.163	0.264	0.177	0.087	0.220	0.180	0.040
0.80	-1.395	0.253	0.172	0.091	0.212	0.180	0.030
0.85	-1.627	0.238	0.173	0.095	0.206	0.181	0.025
0.90	-1.860	0.224	0.171	0.093	0.198	0.181	0.017
0.95	-2.092	0.209	0.172	0.097	0.190	0.181	0.009
1.00	-2.324	0.181	0.181	0.000	0.181	0.181	0.000

TABLE B-14 SECTION DIMENSIONS AS FUNCTIONS OF NON DIMENSIONAL DISTANCE FROM L.L. $r/R = 0.9$

x'	x (ft)	y_u (ft)	y_l (ft)	y_{u-l} (ft)	$(y_u+y_l)/2$ (ft)	n.t. (ft)	y_c (ft)
0.000	2.373	0.168	0.168	0.000	0.168	0.168	0.000
0.0125	2.314	0.184	0.164	0.020	0.174	0.168	0.006
0.025	2.254	0.188	0.164	0.025	0.176	0.168	0.007
0.050	2.136	0.194	0.162	0.032	0.178	0.169	0.009
0.075	1.017	0.196	0.164	0.022	0.175	0.169	0.006
0.100	1.898	0.202	0.115	0.037	0.184	0.169	0.014
0.15	1.661	0.217	0.164	0.053	0.191	0.170	0.021
0.20	1.424	0.225	0.167	0.058	0.196	0.170	0.026
0.25	1.186	0.233	0.167	0.066	0.200	0.171	0.029
0.30	0.949	0.237	0.166	0.071	0.202	0.172	0.030
0.35	0.712	0.240	0.167	0.073	0.204	0.172	0.031
0.40	0.474	0.241	0.169	0.072	0.205	0.173	0.032
0.45	0.237	0.242	0.170	0.072	0.206	0.173	0.033
0.50	0.000	0.240	0.171	0.069	0.206	0.174	0.032
0.55	-0.238	0.240	0.170	0.070	0.205	0.175	0.030
0.60	-0.475	0.242	0.170	0.072	0.206	0.175	0.031
0.65	-0.713	0.242	0.172	0.070	0.207	0.176	0.031
0.70	-0.950	0.237	0.173	0.066	0.206	0.176	0.030
0.75	-1.187	0.236	0.174	0.062	0.205	0.177	0.028
0.80	-1.425	0.231	0.174	0.057	0.203	0.178	0.025
0.85	-1.662	0.222	0.175	0.047	0.199	0.178	0.020
0.90	-1.899	0.215	0.176	0.039	0.196	0.179	0.017
0.95	-2.137	0.200	0.174	0.026	0.187	0.179	0.008
1.00	-2.374	0.180	0.180	0.000	0.180	0.180	0.000

TABLE B-15 SECTION DIMENSIONS AS FUNCTIONS OF NON DIMENSIONAL DISTANCE FROM L.E. $r/R = 1.0$

x'	\bar{x} (ft)	y_u (ft)	y_l (ft)	$y_u - y$ (ft)	$(y_u + y_l)/2$ (ft)	n.t.	y_c (ft)
0.000	2.388	0.172	0.172	0.000	0.172	0.172	0.000
0.0125	2.328	0.184	0.165	0.019	0.175	0.172	0.002
0.025	2.269	0.188	0.162	0.026	0.175	0.172	0.003
0.050	2.150	0.193	0.167	0.026	0.180	0.172	0.008
0.075	2.030	0.197	0.164	0.033	0.181	0.172	0.008
0.100	1.911	0.199	0.164	0.035	0.182	0.173	0.009
0.15	1.673	0.208	0.164	0.044	0.186	0.173	0.013
0.20	1.434	0.215	0.164	0.051	0.190	0.173	0.016
0.25	1.196	0.217	0.165	0.052	0.191	0.174	0.018
0.30	0.958	0.220	0.167	0.053	0.194	0.174	0.020
0.35	0.719	0.223	0.168	0.055	0.196	0.174	0.021
0.40	0.481	0.224	0.169	0.055	0.197	0.174	0.022
0.45	0.242	0.226	0.169	0.057	0.198	0.175	0.023
0.50	0.004	0.227	0.169	0.058	0.198	0.175	0.023
0.55	-0.234	0.226	0.170	0.056	0.198	0.175	0.023
0.60	-0.473	0.225	0.171	0.054	0.198	0.176	0.022
0.65	-0.711	0.227	0.173	0.054	0.200	0.176	0.024
0.70	-0.950	0.224	0.176	0.048	0.200	0.176	0.024
0.75	-1.188	0.220	0.176	0.044	0.198	0.177	0.022
0.80	-1.426	0.216	0.174	0.042	0.195	0.177	0.018
0.85	-1.665	0.209	0.174	0.035	0.192	0.177	0.014
0.90	-1.903	0.202	0.176	0.026	0.189	0.177	0.012
0.95	-2.142	0.195	0.175	0.020	0.185	0.178	0.007
1.00	-2.380	0.178	0.178	0.000	0.178	0.178	0.000

The propeller pitch for the 140 WYTM Cutter Screw is a modification of the K 3-75 pitch. This modification was made to accomodate additional thickness for added strength in the ice fields; the following table compares the pitches P and pitch angles ϕ for the two blades. This data was digitized off the United States Coast Guard Drawing (Fuller 1981 a).

TABLE B-15 PITCH AND PITCH ANGLES

r/R	P (ft)	Standard K 3-75		140 WYTM Cutter		
		$\tan \phi$	ϕ (deg)	P (ft)	$\tan \phi$	ϕ (deg)
0.3	3.70	0.4619	24.79	2.26	0.2821	15.75
0.4	4.40	0.4119	22.38	2.89	0.2706	15.14
0.5	4.92	0.3685	20.23	3.53	0.2644	14.81
0.6	5.51	0.3439	18.98	4.32	0.2696	15.09
0.7	5.95	0.3183	17.66	5.19	0.2777	15.52
0.8	6.38	0.2986	16.63	6.22	0.2912	16.23
0.9	7.21	0.3000	16.70	7.25	0.3017	16.79
1.0	8.36	0.3131	17.38	8.44	0.3161	17.54

APPENDIX C: PROPELLER FORCES

The approximate solution for the angle of zero lift given by the Pankhurst formula (abbott 1959)

$$\alpha_0 = 2/C \sum A y_C$$

is used to obtain the theoretical zero lift angle. The values of A are tabulated in Table C-1, while those of α_0 are tabulated in Table C-2.

TABLE C-1 PANKHURST CONSTANTS

X ¹	A
0.000	1.45
0.025	2.11
0.050	1.56
0.1	2.41
0.2	2.94
0.3	2.88
0.4	3.13
0.5	3.67
0.6	4.69
0.7	6.72
0.8	11.75
0.9	21.72
0.95	99.85
1.00	-104.90

Burriel (1944) presents a correction factor $K\alpha_0$ with which to correct the theoretical zero lift angle to the one found experimentally. The corrected angle α_0 actual is also tabulated in Table C-2. Thickness t and chord are from Table B-8; whereas, the percent of chord at which maximum camber occurs is taken from Tables B-9 through B-15. The factor $K\alpha_0$ is taken from Burris (1944).

TABLE C-2 ZERO LIFT ANGLF

r/R	c (ft)	$\sum A y_c$	α_0 (deg)	t (ft)	t/c	x_{max} %	K_{α_0}	α_0 arct(deq)
0.4	3.607	7.8273	4.34	0.362	0.100	50	0.888	3.85
0.5	3.929	7.3582	3.74	0.301	0.077	50	0.890	3.33
0.6	4.098	6.0459	2.95	0.236	0.058	50	0.890	2.63
0.7	4.475	3.9002	1.74	0.161	0.036	50	0.890	1.55
0.8	4.645	2.7067	1.16	0.115	0.025	50	0.890	1.03
0.9	4.747	2.1996	0.93	0.073	0.015	45	0.905	0.84
1.0	4.768	1.7340	0.73	0.058	0.012	50	0.890	0.65

The ship speed $V_s = 6$ knots, the RPM = $N = 270$ rpm, and the wake reduction factor $W = 0.177$ at $r/R = 0.6$, and the shaft horsepower SHP = 2500 hp are from United States Coast Guard notes (Fuller 1981b). With the usual design process each blade section would have seen an axial velocity V_a , where:

$$\begin{aligned}V_a &= (1 - W) V_s \\&= 0.823 * 6 \text{ kts} \\&= 4.938 \text{ kts} \\V_a &= 8.340 \text{ ft/sec}\end{aligned}$$

However, as discussed in the body of the text this axial velocity is multiplied by a factor V_{ax}/V_a to account for the experimentally determined velocity profile in the nozzle at the location of the screw (Van Manen 1962). From Appendix A the nozzle chord length = 4.282 ft. and the screw diameter D is 8.50 feet. The values of V_{ax}/V_a in Table C-3 are for a 1/D ratio of 0.50 and were obtained from Van Manen 1962. The rotational velocity V_{rot} is given by

$$V_{rot} = 2 \pi n$$

where $n = 270 \text{ rpm}/60 \text{ sec/min} = 4.5 \text{ rps}$. The velocity V is the incident velocity that the blade section sees;

$$V = (V_{ax}^2 + V_{rot}^2)^{1/2}$$

it comes at the blade from an angle β where

$$\beta = \arctan (V_{ax}/V_{rot})$$

TARLF C-3 INCIDENT VELOCITIES AND RESULTANT ANGLE β

r/R	V_{ax}/V_a (ft/sec)	V_{ax} (ft/sec)	V_{rot} (ft/sec)	V (ft/sec)	β (deg)
0.3	0.76	6.34	36.05	36.60	9.97
0.4	0.80	6.67	48.07	48.53	7.90
0.5	0.84	7.01	60.08	60.49	6.65
0.6	0.90	7.51	72.10	72.49	5.94
0.7	0.96	8.01	84.12	84.50	5.44
0.8	1.06	8.84	96.13	96.54	5.25
0.9	1.20	10.01	108.15	108.61	5.29
1.0	1.35	11.26	120.17	120.69	5.35

Figure C-1 shows the relationship between these velocities, β , and the pitch angle ϕ .

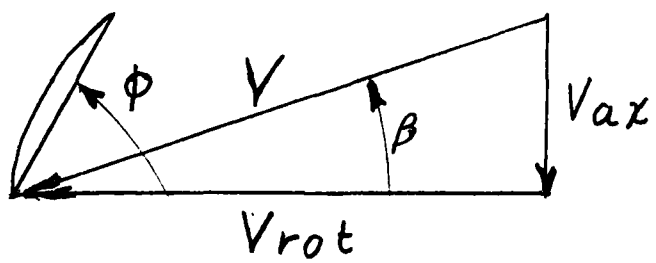


FIGURE C-1 INCIDENT VELOCITIES

For computational purposes it is useful to work with an angle ϕ_0 defined by

$$\phi_0 = \phi + \alpha_{nt} + \alpha_{0act}$$

where

$$\alpha_{nt} = \arctan [(Y_{LE} - Y_{TE})/C]$$

The angle α_0 is the pitch angle of the nose to tail line; it is tabulated in Table C-4.

TABLE C-4 PITCH ANGLE ϕ_0

r/R	ϕ (deg)	C(ft)	Y_{LE} (ft)	Y_{TE} (ft)	$\alpha_{n.t}$ (deg)	α_0 (deg)	ϕ_0
0.4	15.14	3.607	0.198	0.204	-0.10	3.85	18.8
0.5	14.81	3.929	0.193	0.192	0.01	3.33	18.1
0.6	15.09	4.098	0.191	0.180	0.15	2.63	17.8
0.7	15.5?	4.425	0.181	0.184	-0.04	1.55	17.0
0.8	16.23	4.645	0.178	0.181	-0.04	1.03	17.2
0.9	16.79	4.747	0.168	0.180	-0.14	0.84	17.4
1.0	17.54	4.768	0.172	0.178	-0.07	0.65	18.1

The pitch angle ϕ is from Table B-15; the chord c is from Table B-8; Y_{LE} and Y_{TE} are from Tables B-9 through B-15; and α_{0act} is from Table C-2.

Our first empirical correction is to account for the cascade effect. This appears as a correction to the pitch angle ϕ_0 ; though, it is an actual correction to the angle of zero lift. The corrected pitch angle ϕ_0 or is given by

$$\phi_0 \text{ cascade} = \phi_0 - K \alpha_0 * \alpha_0 \text{ act} \quad (C.1)$$

where the correction factor $K \alpha_0$ is a function of β_I , an angle which is initially undetermined and σ . The values of $K \alpha_0$ are found in Burrl 1944. If V denotes the resultant velocity and w the induced downwash, then Figure C-3 shows the relationship between the various velocities and β_I .

$$\sigma = 3 c / (\pi D r/R) \quad (C.2)$$

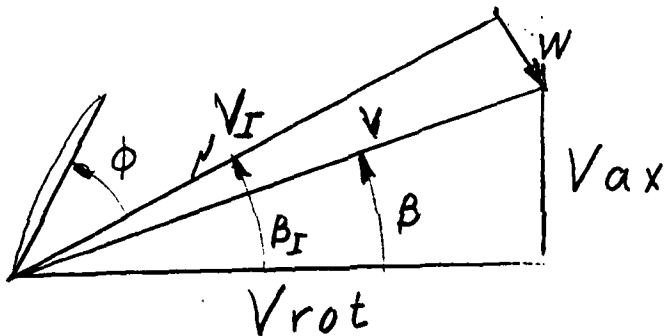


FIGURE C-2 SECTION INDUCED VELOCITY

The determination of ϕ_0 cascade is part of the total iterative process to determine the induced downwash w . In order to start the process β_I is initially assumed to be equal to β . ϕ_0 cascade is calculated based on this value, and the induced angle of attack α_I can be taken as ϕ_0 cascade - β . Figure C.4 shows the relationship between the induced angle of attack, the angle of zero lift α_0 , and the angle of attack of the blade α .

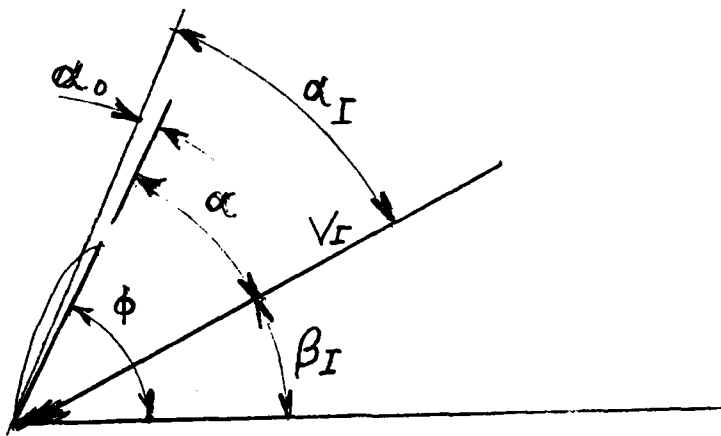


FIGURE C.3 INDUCED ANGLE OF ATTACK

Rather than solve for the downwash w , the iterative scheme is based on solving for α_I . From Figure C-5

$$\beta_I = \phi_0 - \alpha_I$$

However, β_I should be defined in terms of the corrected pitch angle ϕ_0 cascade in place of the pitch angle ϕ_0 ; hence, our β_I is given by

$$\beta_I = \phi_0 \text{ cascade} - \alpha_I \quad (C.3)$$

The induced angle α_I can be expressed in terms of β_I ; Burril (1944) gives the following expression for α_I

$$\alpha_I = \frac{360 K_\epsilon}{\pi^2 K_{g5} K_{s\sigma}} \sin \beta_I \tan (\beta_I - \beta) \left[1 - \frac{\tan(\beta_I - \beta)}{\tan \beta_I} (1 - K\beta_I) \right] \quad (C.4)$$

The factor K_ϵ accounts for a spanwise elliptic distribution. Langan and Wang (1972) show comparisons of experimental and theoretical lift distributions; the elliptic distribution is good for $r/R < 0.95$ but for greater values deviates noticeably from the experimental results. For $r/R > 0.95$ the lift distribution is greater than or equal to the $r/R = 0.95$ value, and the value at $r/R = 0.95$ is a good approximation to the average lift distribution. Moreover, for a ducted propeller there is even less likelihood that the distribution would decrease to zero like an elliptic distribution at the tip. Since we will be using a numerical integration scheme to determine the thrust and since the lift distribution over the tip region is better represented by the lift distribution at $r/R = 0.95$, the value of K_ϵ for $r/R = 0.95$ is used for the value of K_ϵ at $r/R = 1$. K_ϵ is a function of the angle ϵ :

$$\epsilon = \beta_I + (\beta_I - \beta) \quad (C.5)$$

$K_{\beta I}$ is the Goldstein correction factor for a three bladed propeller. K_s is a slope correction factor and K_{gs} is an additional cascade correction factor. These factors are to be found in Burril (1944).

Equations (C.1) thru (C.5) form the basis for an iterative scheme to determine α_I , β_I , and ϕ_0 cascade. To start the scheme assume $\beta_I = \beta$ and compute ϕ_0 cascade use (C.2) to get a starting value for α_I or use a value of α_I between -5° and 15° . In either case use (C.3) to compute β_I and (C.4) to compute α_I out. If this value does not agree with the starting value of α_I , use it for a new value of $\alpha_{I\text{in}}$ (i.e. α_I going into the iteration) provided it lies in the range -5° to 15° ; otherwise, use another angle out of this range. Compare the new $\alpha_{I\text{out}}$ with the $\alpha_{I\text{in}}$. A good common sense choice of $\alpha_{I\text{in}}$ quickly develops, and convergence occurs rapidly. There is no need to change ϕ_0 cascade or the K 's for each new β_I ; simply wait for convergence with the wrong set of K 's and then adjust the K 's and ϕ_0 cas. for the new β_I . After the first few times through there is little change in these factors.

Table C-5 shows the final results for ϕ_0 cascade and Table C-6 presents the final iterative results for α_I .

TABLE C-5 CORRECTED PITCH ANGLE

r/R	σ	β_I (deg)	$K_g \alpha_0$	α_0 act	ϕ_0 (deg)	ϕ_0 cas. (deg)
0.4	1.01	14.98	0.43	3.85	18.89	17.24
0.5	0.88	14.30	0.36	3.33	18.15	16.96
0.6	0.77	14.29	0.28	2.63	17.87	17.14
0.7	0.72	14.12	0.24	1.55	17.03	16.66
0.8	0.65	14.68	0.20	1.03	17.22	17.02
0.9	0.59	15.79	0.15	0.84	17.49	17.36
1.0	0.54	16.95	0.13	0.65	18.12	18.03

Equation C-2 is used to compute σ from the values of c in Table C-4. $D = 8.50$ ft. The hydrodynamics pitch angle β_I comes out of the iteration; the values in the table are the final values. $K_g \alpha_0$ is from Burril (1944), α_0 act is from Table C-2 and ϕ_0 from Table C-4.

The final values of the factors which enter into the iterative calculation of Equation C-4 are tabulated in Table C-6.

The theoretical lift coefficient $2\pi\alpha_I$ needs an experimental correction K_s and a cascade correction; the corrected lift coefficient C_L' is given by:

$$C_L' = 2\pi K_s K_{gs} \alpha_I \text{ (rad)}$$

These corrections can be thought of as corrections to the slope, thus the subscript s.

There are three components to the drag coefficient. Burril (1944) gives the minimum drag component in terms of the following empirical formula:

TABLE C-6 INDUCED ANGLE OF ATTACK

r/R	$\beta_I(\text{deg})$	σ	$\epsilon(\text{deg})$	K_ϵ	K_s	K_{qs}	K_{gI}	$\alpha_{I\text{out}}(\text{deg})$	$\alpha_{I\text{in}}(\text{deg})$	$\alpha_I(\text{deg})$
0.4	14.98	1.01	-0.05	0.98	0.935	0.53	0.98	2.2622	2.2625	2.26
0.5	14.30	0.88	21.95	0.98	0.945	0.53	0.98	2.6543	2.6544	2.65
0.6	14.29	0.77	22.64	0.92	0.950	0.58	0.98	2.8433	2.8434	2.84
0.7	14.12	0.72	22.82	0.83	0.950	0.63	0.94	2.5319	2.5320	2.53
0.8	14.68	0.65	24.09	0.68	0.950	0.64	0.83	2.3446	2.3446	2.34
0.9	15.79	0.59	26.29	0.45	0.950	0.69	0.60	1.5721	1.5720	1.57
1.0	16.95	0.54	28.54	0.30	0.950	0.73	0.43	1.0855	1.0865	1.08

$$C_{D_{\min}} = 0.0056 + 0.01 t/c + 0.10 (t/c)^2 + K_2$$

where the constant K_2 can be determined from Figure C-9. The values of K_2 in Table C-7 were obtained through linear interpolation. A second factor

$$\Delta C_{Dg} = \frac{\pi}{180} \tan(\beta_I - \beta) C_L$$

is the induced drag component. The third component is a component depending on how close to optimal lift the section is operating.

$$\Delta C_D = K_3 (C_L^2 - C_{L_{\text{opt}}}^2)$$

This component would be zero at optimal lift $C_{L_{\text{opt}}}$; given together with K_3 Burril as a function of maximum camber and thickness to chord ratio. There is a correction to lift due to the drag; Burril gives this correction as

$$\delta C_L = \frac{K_{gs}}{2} C_D \tan(\beta_I - \beta)$$

Table C-7 presents the values of all these lift and drag components together with the final lift and drag coefficients. α_I in radian is used in computing C_L ; otherwise, the table is straight forward.

Now the incremental lift $dL = \frac{1}{2} \rho V_I^2 c C_L$ is perpendicular to the line of action of the resolent velocity V_I , and the incremental drag $dD = \frac{1}{2} \rho V_I^2 c C_D$ has the same direction. Figure C-5. The incremental

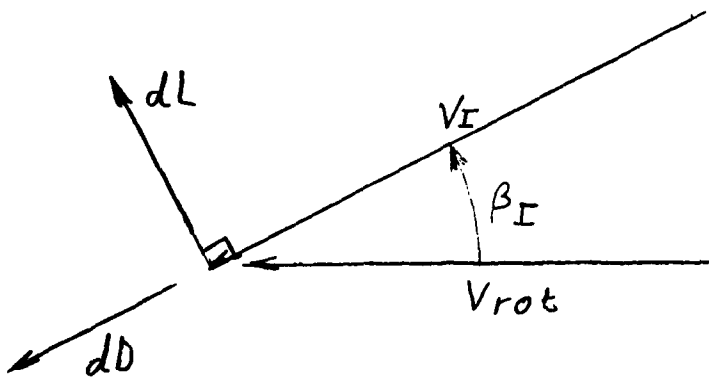


Figure C-4 LIFT AND DRAG ORIENTATION

thrust dT and the tangential force dQ/r are related to dL and dD by:

$$dT = dL \cos \beta_I - dD \sin \beta_I$$

$$\frac{dQ}{r} = dL \sin \beta_I + dD \cos \beta_I$$

TABLE C-7 LIFT AND DRAG COEFFICIENTS

r/R	α_1 (deg)	K_s	K_{qs}	t/c	y_{cmax} (ft)	$C(f_t)$	y_{cmax}/c	K_2	K_3	C_{Lopt}
0.4	2.26	0.935	0.53	0.100	0.157	3.607	0.042	0.00200	0.00696	0.03
0.5	2.65	0.945	0.53	0.077	0.126	3.929	0.032	0.00154	0.00635	0.26
0.6	2.84	0.950	0.58	0.058	0.099	4.098	0.024	0.00109	0.00536	0.20
0.7	2.53	0.950	0.63	0.036	0.070	4.475	0.016	0.00066	0.00534	0.20
0.8	2.34	0.950	0.64	0.025	0.049	4.645	0.011	0.00045	0.00503	0.06
0.9	1.57	0.950	0.69	0.015	0.032	4.747	0.007	0.00029	0.00480	0.03
1.0	1.08	0.950	0.73	0.012	0.023	4.768	0.005	0.00021	0.00480	0.02

r/R	C_{Dmin}	β_I (deg)	β (deg)	C'_L	∇C_D	∇C_D	C_D	δC_L	δC_L	C_L
0.4	0.00960	14.98	7.90	0.1228	0.00027	0.00022	0.01008	0.00033	0.00033	0.1231
0.5	0.00851	14.30	6.65	0.1455	0.00034	0.00008	0.00893	0.00032	0.00032	0.1459
0.6	0.00760	14.29	5.94	0.1716	0.00044	0.00000	0.00804	0.00034	0.00034	0.1719
0.7	0.00675	14.12	5.44	0.1661	0.00044	0.00001	0.00720	0.00035	0.00035	0.1664
0.8	0.00636	14.68	5.25	0.1560	0.00045	0.00005	0.00686	0.00036	0.00036	0.1564
0.9	0.00606	15.79	5.29	0.1128	0.00036	0.00003	0.00646	0.00041	0.00041	0.1133
1.0	0.00594	16.95	5.35	0.0821	0.00029	0.00002	0.00625	0.00047	0.00047	0.0826

The total propeller thrust is

$$T = Z \int_{\text{root}}^{\text{tip}} dT$$

where Z is the number of blades,
or in terms of the discrete values in this report

$$T = 3 * 0.1R \sum dT$$

Similarly, the total torque is given by

$$Q = Z \int_{\text{root}}^{\text{tip}} dQ,$$

or

$$Q = 3 * 0.1R \sum dQ$$

Results based on these formulae are presented in Table C-8. These results are computed for a water density $\rho = 1.94 \text{ lb sec}^2/\text{ft}^4$. The values of dT , dQ/r , and dQ for $r/R = 1.0$ have been cut in half to reflect that the interval over which these increments act is half the size of the other intervals. The interval t around $r/R = 0.4$ enters fully into the calculation; however, the blade for $r/R < 0.35$ to the hub has been neglected. Note that the propeller hub has a 1.0625 foot radius which corresponds to an $r/R = 0.25$. By neglecting the portion of the blade inboard of $r/R = 0.35$ we are then neglecting $0.425' = 5.1"$ of the blade. Within this segment the hydrodynamics is not as straight forward. As can be seen from the results at $r/R = 0.4$, the loading is small, and the results will not change significantly.

TABLE C-8 PROPELLER FORCES

r/R	$\beta_1(\text{deg})$	c_L	c_D	$dL(1\text{bs}/\text{ft})$	$dD(1\text{bs}/\text{ft})$	$dT(1\text{bs}/\text{ft})$	$d0/r(1\text{bs}/\text{ft})$	$dQ/1\text{bs}$
0.4	14.98	0.1231	0.0101	1015	83	959	342	1456
0.5	14.30	0.1459	0.0089	2034	124	1940	623	2648
0.6	14.29	0.1719	0.0080	3592	168	3439	1049	4460
0.7	14.12	0.1664	0.0072	5157	223	4947	1474	6267
0.8	14.68	0.1564	0.0068	6567	288	6279	1942	8257
0.9	15.79	0.1133	0.0064	6153	351	5825	2012	8550
1.0	16.95	0.0826	0.0062	5565	421	2600	2600	4304

$$\rho = 1.94 \text{ lb sec}^2/\text{ft}^4$$

$$T = 33136 \text{ lbs}$$

$$n = 45825 \text{ ft lbs}$$

$$\sum dT = 25989$$

$$\sum d0 = 35940$$

The velocity distribution is obtained using the Goldstein (1952) approximation. In this method the velocity on the surface is given by

$$v = \frac{e^{C_0} (1 + \epsilon')}{(\psi^2 + \sin^2 \phi)}^{1/2} \left| \left(1 - \frac{C_L^2}{a_0^2} \right)^{1/2} \sin (\phi + \epsilon + \beta) - \frac{C_L}{a_0} \cos (\phi + \epsilon + \beta) + \frac{C_L}{2\pi e^{C_0}} \right| \quad (C.6)$$

where ϕ and ψ are transform plane coordinates given by

$$x = 1/2 C (1 + \cos \phi)$$

$$y = 1/2 C \psi (\phi) \sin \phi$$

The angle $\epsilon (\phi)$ is given explicitly in this approximation by

$$\epsilon (\phi) = (1/2\pi) \rho \int_0^{2\pi} \psi (t) \cot 1/2 (\phi-t) dt, \quad (C.7)$$

C_0 is a constant for each section, and it is given by

$$C_0 = 1/2 (\pi/2) \int_0^{2\pi} \psi (\phi) d\phi \quad (C.8)$$

If β satisfies the condition

$$\left(1 - \frac{C_L^2}{a_0^2} \right)^{1/2} \sin (\epsilon + \beta) - \frac{C_L}{a_0} \cos (\epsilon + \beta) + \frac{C_L}{2\pi e^{C_0}}, \quad (C.9)$$

the Kutta-Joukowski condition is satisfied. C_L is the left coefficient from Table C-7, and a_0 is the left slope corrected for viscosity; $a_0 = 2\pi K_s$ where K_s is from Table C-6.

β is determined through an iterative solution of Equation (C.9). C_0 , the angle ϵ , and its derivative ϵ' are computed through the methods suggested by Thwaites (1960). The results for sections at $r/R = 0.5, 0.7$, and 0.9 are presented in Table C-9 through Table C-11.

TABLE C-9 SECTION RELOCITY DISTRIBUTION AND PRESSURE COEFFICIENTS FOR $r/R = 0.5$,
 $C_L = 0.146$

x/c	x (ft)	$(v/\eta)_u$	$(C_p)_u$	$(v/\eta)_l$	$(C_p)_l$
0	0	0	1	0	1
0.006	0.024	0.414	0.828	1.292	-0.670
0.024	0.096	0.740	0.453	1.257	-0.580
0.054	0.214	0.870	0.243	1.109	-0.230
0.095	0.375	0.927	0.141	1.050	-0.104
0.146	0.576	0.977	0.046	1.003	-0.006
0.206	0.810	1.061	-0.125	0.993	0.013
0.273	1.073	1.080	-0.167	0.982	0.035
0.345	1.358	1.119	-0.252	0.975	0.050
0.422	1.657	1.112	-0.236	0.957	0.083
0.500	1.965	1.130	-0.213	0.962	0.074
0.578	2.272	1.121	-0.257	0.956	0.085
0.654	2.572	1.105	-0.221	0.950	0.097
0.727	2.857	1.118	-0.249	0.932	0.132
0.793	3.120	1.118	-0.250	0.925	0.144
0.854	3.354	1.058	-0.119	0.940	0.116
0.904	3.555	1.000	0.000	0.941	0.115
0.946	3.716	0.975	0.049	0.924	0.147
0.976	3.834	0.892	0.204	0.863	0.254
0.991	3.906	0.798	0.362	0.787	0.380
1.000	3.930	0	1	0	1

TABLE C-10 SECTION VELOCITY DISTRIBUTION AND PRESSURE COEFFICIENTS FOR $r/R = 0.7$,
 $C_L = 0.166$

x/c	$x(\text{ft})$	$(v/V)u$	$(C_p)u$	$(v/V)l$	$(C_p)l$
0	0	0	1	0	1
0.006	0.028	0.873	0.239	0.980	0.621
0.024	0.109	1.005	-0.010	1.079	-0.163
0.054	0.244	1.090	-0.188	0.988	0.023
0.095	0.427	1.071	-0.147	0.963	0.073
0.146	0.655	1.089	-0.187	0.981	0.037
0.206	0.922	1.078	-0.164	0.978	0.043
0.273	1.222	1.083	-0.191	0.971	0.057
0.345	1.546	1.037	-0.218	0.966	0.066
0.422	1.888	1.114	-0.242	0.965	0.069
0.500	2.238	1.045	-0.091	0.958	0.082
0.578	2.588	1.112	-0.237	0.975	0.050
0.654	2.930	1.023	-0.047	0.942	0.112
0.727	3.254	1.013	-0.026	0.961	0.076
0.793	3.553	1.794	0.369	0.945	0.106
0.854	3.820	0.846	0.285	0.983	0.033
0.904	4.048	1.322	-0.741	0.961	0.077
0.946	4.232	1.054	-0.110	0.995	0.009
0.976	4.366	0.991	0.018	0.933	0.129
0.994	4.448	0.882	0.221	0.889	0.209
1.000	4.476	0	1	0	1

TABLE C-111 SECTION BELOCITY DISTRIBUTION AND PRESSURE COEFFICIENTS FOR $r/R = 0.9$, $C_L = 0.113$

x/c	$x(fft)$	$(v/v)u$	$(C_p)u$	$(v/v)^T$	$(C_p)^T$
0	0	0	1	0	1
0.006	0.029	0.792	0.373	1.102	-0.214
0.024	0.116	0.994	0.012	1.011	-0.022
0.054	0.259	0.978	0.044	0.979	-0.042
0.095	0.453	0.965	0.069	1.010	-0.021
0.146	0.695	1.025	-0.051	0.976	0.046
0.206	0.978	1.023	-0.047	0.997	0.006
0.273	1.296	1.034	-0.068	0.980	0.037
0.345	1.640	1.034	-0.070	0.976	0.046
0.422	2.002	1.034	-0.070	0.978	0.043
0.500	2.374	1.020	-0.041	0.978	0.044
0.578	2.745	1.030	-0.061	0.962	0.074
0.654	3.108	1.043	-0.087	0.966	0.068
0.727	3.452	1.044	-0.090	0.967	0.064
0.793	3.769	1.047	-0.096	0.953	0.082
0.854	4.053	1.035	-0.072	0.964	0.071
0.904	4.295	1.044	-0.091	0.919	0.155
0.946	4.489	1.077	-0.161	0.910	0.172
0.976	4.632	1.028	-0.058	0.951	0.095
0.994	4.719	1.108	-0.227	0.871	0.241
0	4.748	0	1	0	1

From the Bernulli equation

$$p_{atm} + \frac{1}{2} \rho V^2 + \gamma h = p_{atm} + p_1 + \frac{1}{2} \rho v^2 + \gamma h$$

where p_1 is the local gage pressure on the foil minus the static head. $\gamma = 62.4$ lbs/ft² is the specific weight of fresh water, and $p_{atm} = 14.7$ psi = 2116.8 psf is the standard atmospheric pressure. $\rho = 1.94$ lb sec/ft³. The water depth h will be taken as the depth of the propeller axis below the design water line, 7.5 feet, minus the section radius.

$$h = 7.5' - r$$

The local pressure p_1 in terms of the local velocity v is given by

$$p_1 = \frac{1}{2} \rho (V^2 - v^2);$$

a local pressure coefficient C_p can be defined by

$$C_p = p_1 / \frac{1}{2} \rho V^2 = 1 - (v/V)^2 \quad (C.10)$$

Values of the pressure coefficient for $r/R = 0.5, 0.7,$ and 0.9 may be found in Tables C-9 through C-11.

For cavity free operation the local absolute pressure must exceed the vapor pressure e , that is

$$p_{atm} + p_1 + \gamma h > e$$

or

$$C_p > \frac{e - p_{atm} - \gamma h}{\frac{1}{2} \rho V_a^2} \quad (C.11)$$

Our analysis of cavitation is based on a summer time operating temperature of 70° F; at this temperature $e = 0.36$ pse = 51.8 psf. Table C-12 presents conditions that the pressure coefficient must meet for cavity free operation. The velocities V are from Table C-3.

TABLE C-12 CAVITATION CRITERIA

r/R	γh (psf)	$e - \gamma h - p_{atm}$ (psf)	V (ft/sec)	$\frac{1}{2} \rho V^2$ (psf)	$C_p >$
0.5	335.4	-2400	60.49	3549	-0.676
0.7	282.4	-2347	84.50	6926	-0.339
0.9	229.3	-2294	108.61	11442	-0.200

Cavitation occurs at the face side of the leading edge at $r/R=0.9$ to $r/R=0.5$; although the actual value of C_p at $r/R=0.5$ is not below the critical value, it is very marginal. Cavitation also occurs on the back side at $r/R=0.7$.

APPENDIX D: STRUCTURAL ANALYSIS OF THE BLADE UNDER ICE LOADING

As mentioned previously ice loading is difficult to predict; as before, the criterion proposed by Graft (1977) is used. The blade should be able to support a load equal to the crushing strength of the ice times the appropriate projected area. The rotating blade could be crushing through an ice chunk in the way of its rotational motion; in this case the projected area is in a radial plane that is a plane containing the axis of the shaft and a radial line. Ice could be forced against the blade in a forward or aft direction, in which case the projected area of the blade would be the appropriate area to use; however, in our analysis the developed area is used for convenience of calculation. The substitution of developed for projected area is slightly conservative in terms of predicted loading and stresses.

Tables D-1 through D-3 present the section properties for $r/R=0.4, 0.6,$ and 0.8 . The first eight columns of each table correspond to the respective column in Table A-1. I_x is the moment of inertia around the centroidal axis parallel to the chord. The remaining columns are used to obtain \bar{x} , I_y , and I_{xy} , where I_y is the moment of inertia around the remaining centroidal axis.

$$\bar{x} = \frac{1}{A} \int_{L.E.}^{T.E.} x \, dA$$

$$= 0.05 C/A \sum (y_u - y_l)$$

$$I_y = \frac{1}{A} \int_{L.E.}^{T.E.} (x - \bar{x})^2 \, dA$$

$$= 0.05C \sum (x - \bar{x})^2 (y_u - y_l)$$

and

$$I_{xy} = 0.05C \sum (x - \bar{x})(y - \bar{y})(y_u - y_l)$$

Table D-4 presents the corresponding data for an NACA 0018 symmetric foil section with a 1.5 ft chord. Only y_u is given since $y_l = -y_u$. Also \bar{y}_i for each section is 0 as is \bar{y} ; thus, $(y_l - \bar{y}) \, dA$ is also zero. I_x is dependent solely on $\sum I_i$.

TABLE D-1a SECTION PROPERTIES r/R=0.4

x'	$y_u - y_1$ (ft)	\bar{y}_1 (ft)	$\bar{y}_1^* (y_u - y_1) (ft)^2$	$\bar{y}_1 \bar{y}$ (ft)	$(y_u - y_1) (\bar{y}_1 - y) ft^2$	$(y_u - y_1) (\bar{y}_1 - y)^2 (ft)^3$	$\bar{I}_1 (ft^4)$
0.000	0	0.198	0.000	-0.122	0.000	0.0000	0.000
0.05	0.119	0.239	0.028	-0.082	-0.010	0.0008	0.000
0.10	0.179	0.267	0.048	-0.054	-0.010	0.0005	0.000
0.15	0.233	0.291	0.068	-0.030	-0.007	0.0002	0.000
0.20	0.279	0.307	0.086	-0.014	-0.004	0.0001	0.000
0.25	0.315	0.324	0.102	0.003	0.001	0.0000	0.000
0.30	0.338	0.337	0.114	0.017	0.006	0.0001	0.000
0.35	0.351	0.346	0.121	0.025	0.009	0.0002	0.000
0.40	0.360	0.348	0.125	0.028	0.010	0.0003	0.000
0.45	0.362	0.350	0.127	0.030	0.011	0.0003	0.000
0.50	0.362	0.353	0.128	0.033	0.012	0.0004	0.000
0.55	0.353	0.346	0.122	0.025	0.009	0.0002	0.000
0.60	0.344	0.338	0.116	0.018	0.006	0.0001	0.000
0.65	0.321	0.333	0.107	0.012	0.004	0.0000	0.000
0.70	0.299	0.323	0.096	0.022	0.001	0.0000	0.000
0.75	0.271	0.306	0.083	-0.015	-0.004	0.0001	0.000
0.80	0.231	0.287	0.066	-0.034	-0.008	0.0003	0.000
0.85	0.183	0.270	0.049	-0.051	-0.009	0.0005	0.000
0.90	0.130	0.249	0.032	-0.071	-0.109	0.0007	0.000
0.95	0.076	0.228	0.017	-0.092	-0.007	0.0006	0.000
1.00	0	0.204	0.000	-0.116	0.000	0.0000	0.000
Σ	5.106	-----	1.636	-----	0.000	0.0054	0.046

$$A = 0.921 \text{ ft}^2$$

$$\bar{y} = 0.320 \text{ ft}$$

$$I_x = 0.0082 \text{ ft}^4 = 170 \text{ in}^4$$

TABLE D-1b SECTION PROPERTIES $r/R=0.4$

x'	$x(y_u-y_1)(ft)^2$	$\bar{x}-x(ft)$	$(y_u-y_1)(\bar{x}-x)ft^2$	$(y_u-y_1)(x-x)ft^2$	$(y_u-y_1)(x-x)^2(ft)^3$	$(y_u-y_1)(x-x)(y-y)(ft^3)$
0.00	0.000	1.736	0.000	0.000	0.000	0.000
0.05	0.199	1.555	0.185	0.288	-0.015	-0.015
0.10	0.267	1.375	0.246	0.338	-0.013	-0.013
0.15	0.305	1.194	0.278	0.332	-0.008	-0.008
0.20	0.315	1.014	0.283	0.287	-0.004	-0.004
0.25	0.299	0.834	0.263	0.219	0.001	0.001
0.30	0.260	0.653	0.221	0.144	0.004	0.004
0.35	0.207	0.473	0.166	0.078	0.004	0.004
0.40	0.147	0.293	0.105	0.031	0.003	0.003
0.45	0.082	0.112	0.041	0.004	0.001	0.001
0.50	0.017	-0.068	-0.025	0.002	-0.001	-0.001
0.55	-0.047	-0.248	-0.088	0.022	-0.002	-0.002
0.60	-0.108	-0.429	-0.148	0.063	-0.003	-0.003
0.65	-0.158	-0.609	-0.196	0.119	-0.002	-0.002
0.70	-0.202	-0.789	-0.236	0.186	-0.000	-0.000
0.75	-0.232	-0.970	-0.263	0.255	0.004	0.004
0.80	-0.239	-1.150	-0.266	0.306	0.009	0.009
0.85	-0.222	-1.330	-0.244	0.324	0.012	0.012
0.90	-0.181	-1.511	-0.196	0.297	0.014	0.014
0.95	-0.120	-1.691	-0.128	0.217	0.012	0.012
1.00	-0.000	-1.872	-0.000	0.000	0.000	0.000
Σ	0.590	-----	0.000	3.513	0.015	0.015

$$\bar{x} = 0.115 \text{ ft}$$

$$I_y = 13140 \text{ in}^4$$

$$I_{xy} = 55 \text{ in}^4$$

TABLE D-2a SECTION PROPERTIES $r/R=0.6$

x'	$y_u - y_1$ (ft)	\bar{y}_1 (ft)	$\bar{y}_1^* (y_u - y_e) (ft)^2$	$\bar{y}_1 - y$ (ft)	$(y_u - y_1) (\bar{y}_1 - y)^2$	$(y_u - y_1) (\bar{y}_1 - y)^2 (ft)^3$	I_1 ft ³
0.000	0	0.191	0.000	-0.071	0.000	0.0000	0.0000
0.05	0.092	0.206	0.019	-0.056	-0.005	0.0003	0.0001
0.10	0.125	0.223	0.028	-0.040	-0.005	0.0002	0.0002
0.15	0.150	0.235	0.035	-0.027	-0.004	0.0001	0.0003
0.20	0.169	0.248	0.042	-0.015	-0.003	0.0000	0.0004
0.25	0.185	0.260	0.048	-0.003	-0.001	0.0000	0.0005
0.30	0.205	0.269	0.055	0.006	0.001	0.0000	0.0007
0.35	0.220	0.276	0.061	0.014	0.003	0.0000	0.0009
0.40	0.231	0.281	0.065	0.018	0.004	0.0001	0.0010
0.45	0.234	0.283	0.066	0.021	0.005	0.0001	0.0011
0.50	0.236	0.285	0.067	0.023	0.005	0.0001	0.0011
0.55	0.230	0.282	0.065	0.020	0.004	0.0001	0.0010
0.60	0.221	0.281	0.062	0.018	0.004	0.0001	0.0009
0.65	0.209	0.277	0.058	0.014	0.003	0.0000	0.0008
0.70	0.193	0.269	0.052	0.006	0.001	0.0000	0.0006
0.75	0.177	0.261	0.046	-0.002	0.000	0.0000	0.0005
0.80	0.152	0.249	0.038	-0.013	-0.002	0.0000	0.0003
0.85	0.128	0.236	0.030	-0.026	-0.003	0.0001	0.0002
0.90	0.098	0.221	0.022	-0.041	-0.104	0.0002	0.0001
0.95	0.065	0.203	0.013	-0.060	-0.004	0.0002	0.0000
1.00	0	0.180	0.000	-0.082	0.000	0.0000	0.0000
Σ	3.320	-----	0.871	0	0.0017	0.0105	

$$C = 4.098 \text{ ft}_2$$

$$A = 0.680 \text{ ft}$$

$$\bar{y} = 0.262 \text{ ft}$$

$$I_x = 0.0025 \text{ ft}^4 = 52 \text{ in}^4$$

TABLE D-2b SECTION PROPERTIES $r/R=0.6$

x'	$x(y_u - y_e) (ft^2)$	$\bar{x}x (ft)$	$(y_u - y_e)(\bar{x} - x) ft^2$	$(y_u - y_e)(x - \bar{x})^2 (ft^3)$	$(y_u - y_e)(x - \bar{x})(y - \bar{y})$
0.00	0.000	1.996	0.000	0.000	0.0000
0.05	0.164	1.791	0.165	0.295	-0.0093
0.10	0.198	1.586	0.198	0.314	-0.0079
0.15	0.206	1.381	0.207	0.286	-0.0057
0.20	0.198	1.176	0.199	0.234	-0.0030
0.25	0.177	0.071	0.180	0.174	-0.0005
0.30	0.156	0.766	0.157	0.120	0.0010
0.35	0.122	0.562	0.124	0.069	0.0017
0.40	0.081	0.357	0.082	0.029	0.0015
0.45	0.034	0.152	0.036	0.005	0.0007
0.50	-0.014	-0.053	-0.012	0.001	-0.0003
0.55	-0.061	-0.258	-0.059	0.015	-0.0012
0.60	-0.104	-0.463	-0.102	0.047	-0.0018
0.65	-0.141	-0.668	-0.140	0.093	-0.0020
0.70	-0.170	-0.873	-0.168	0.147	-0.0010
0.75	-0.192	-1.078	-0.191	0.206	0.0004
0.80	-0.196	-1.282	-0.195	0.250	0.0026
0.85	-0.191	-1.487	-0.190	0.283	0.0050
0.90	-0.166	-1.692	-0.166	0.281	0.0069
0.95	-0.124	-1.897	-0.123	0.234	0.0074
1.00	-0.000	-2.102	-0.000	0.000	0.0000
Σ	-0.020	-----	0.000	3.086	-0.0055

$$\bar{x} = 0.0059 \text{ ft} \quad I_y = 0.632 \text{ ft}^4 = 13110 \text{ in}^4 \quad I_{xy} = -24 \text{ in}^4$$

TABLE D-3a SECTION PROPERTIES $r/R=0.8$

x'	$y_u - y_i$ (ft)	\bar{y}_i (ft)	$\bar{y}_i^* (y_u - y_e)$ (ft) ²	$y_i - \bar{y}$ (ft)	$(y_u - y_e) \bar{y}^2$	$(y_u - y_e) (\bar{y}_i - \bar{y})^2$	I_i (ft ³)
0.00	0.000	0.178	0.000	-0.039	0.000	0.0000	0.0000
0.05	0.042	0.183	0.008	-0.034	-0.001	0.0000	0.0000
0.10	0.055	0.192	0.011	-0.025	-0.001	0.0000	0.0000
0.15	0.066	0.198	0.013	-0.019	-0.001	0.0000	0.0000
0.20	0.076	0.205	0.016	-0.012	-0.001	0.0000	0.0000
0.25	0.085	0.212	0.018	-0.005	-0.000	0.0000	0.0001
0.30	0.097	0.218	0.021	0.001	0.000	0.0000	0.0001
0.35	0.106	0.222	0.024	0.005	0.001	0.0000	0.0001
0.40	0.113	0.226	0.025	0.009	0.001	0.0000	0.0001
0.45	0.113	0.227	0.026	0.010	0.001	0.0000	0.0001
0.50	0.115	0.229	0.026	0.012	0.001	0.0000	0.0001
0.55	0.114	0.225	0.026	0.008	0.001	0.0000	0.0001
0.60	0.109	0.226	0.025	0.009	0.001	0.0000	0.0001
0.65	0.099	0.228	0.023	0.011	0.001	0.0000	0.0001
0.70	0.094	0.226	0.021	0.009	0.001	0.0000	0.0001
0.75	0.087	0.221	0.019	-0.004	0.000	0.0000	0.0001
0.80	0.081	0.213	0.017	-0.004	-0.000	0.0000	0.0000
0.85	0.065	0.206	0.013	-0.011	-0.001	0.0000	0.0000
0.90	0.053	0.198	0.010	-0.019	-0.001	0.0000	0.0000
0.95	0.037	0.191	0.007	-0.026	-0.001	0.0000	0.0000
1.00	0	0.181	0.000	-0.036	0.000	0.0000	0.0000
Σ	1.607	-----	0.348	-----	0.000	0.0002	0.0012

$$C = 4.645 \text{ ft}_2$$

$$A = 0.373 \text{ ft}$$

$$\bar{y} = 0.217 \text{ ft}$$

$$I_x = 0.0003 \text{ ft}^4 = 7 \text{ in}^4$$

TABLE D-3b SECTION PROPERTIES r/R=0.8

x'	$x(y_u - y_e) (ft^2)$	$\bar{x} - x (ft)$	$(y_u - y_e)(x - \bar{x})(ft^2)$	$(y_u - y_e)(x - \bar{x})^2 (ft^3)$	$(y_u - y_e)(x - \bar{x})(y - \bar{y})(ft^3)$
0.00	0.000	2.313	0.000	0.000	0.0000
0.05	0.088	2.080	0.087	0.182	-0.0029
0.10	0.102	1.848	0.102	0.188	-0.0026
0.15	0.107	1.616	0.107	0.172	-0.0020
0.20	0.106	1.384	0.105	0.146	-0.0012
0.25	0.099	1.151	0.098	0.113	-0.0005
0.30	0.090	0.919	0.089	0.082	0.0001
0.35	0.074	0.687	0.073	0.050	0.0004
0.40	0.052	0.455	0.051	0.023	0.0005
0.45	0.026	0.222	0.025	0.006	0.0002
0.50	0.000	-0.010	-0.001	0.000	0.0000
0.55	-0.027	-0.242	-0.028	0.007	-0.0002
0.60	-0.051	-0.474	-0.052	0.025	-0.0005
0.65	-0.069	-0.707	-0.070	0.049	-0.0008
0.70	-0.088	-0.939	-0.088	0.083	-0.0008
0.75	-0.101	-1.171	-0.102	0.119	-0.0004
0.80	-0.113	-1.403	-0.114	0.160	0.0005
0.85	-0.106	-1.636	-0.106	0.174	0.0012
0.90	-0.099	-1.868	-0.099	0.185	0.0019
0.95	-0.077	-2.100	-0.078	0.163	0.0020
1.00	0.000	-2.332	0.000	0.000	0.0000
Σ	0.013	-----	0.000	1.925	-0.0051

$$\bar{x} = 0.0083 ft \quad I_y = 0.447 ft^4 = 9273 \text{ in}^4 \quad I_{xy} = -25 \text{ in}^4$$

TABLE D-4 SECTION PROPERTIES FOR ICF DEFLECTOR STRUT

x'	x (ft)	y_u (ft)	y_{u-y_1} (ft)	I_i (ft)	$x(y_{u-y_1})$ ft	$x-x$ (ft)	$(y_{u-y_1})(x-x)$ (ft ²)	$(y_{u-y_1})(x-x)^2$ ft ³
0.00	0.750	0.000	0.000	0.0000	0.000	0.636	0.000	0.000
0.05	0.675	0.080	0.160	0.0003	0.108	0.562	0.090	0.050
0.10	0.600	0.105	0.211	0.0008	0.126	0.486	0.102	0.050
0.15	0.525	0.120	0.240	0.0012	0.126	0.412	0.099	0.041
0.20	0.450	0.129	0.258	0.0014	0.116	0.336	0.087	0.029
0.25	0.375	0.134	0.267	0.0016	0.100	0.262	0.070	0.018
0.30	0.300	0.135	0.270	0.0016	0.081	0.186	0.050	0.009
0.35	0.225	0.133	0.265	0.0016	0.060	0.112	0.030	0.003
0.40	0.150	0.131	0.261	0.0015	0.039	0.036	0.010	0.000
0.45	0.075	0.125	0.250	0.0013	0.019	-0.038	-0.010	0.000
0.50	0.000	0.119	0.238	0.0011	0.000	-0.114	-0.027	0.003
0.55	-0.075	0.111	0.222	0.0009	-0.017	-0.188	-0.042	0.008
0.60	-0.150	0.103	0.205	0.0007	-0.031	-0.264	-0.054	0.014
0.65	-0.225	0.093	0.185	0.0005	-0.042	-0.338	-0.063	0.021
0.70	-0.300	0.082	0.165	0.0004	-0.050	-0.414	-0.068	0.028
0.75	-0.375	0.071	0.142	0.0002	-0.053	-0.488	-0.069	0.034
0.80	-0.450	0.059	0.118	0.0001	-0.053	-0.564	-0.066	0.037
0.85	-0.525	0.046	0.092	0.0001	-0.048	-0.638	-0.058	0.037
0.90	-0.600	0.033	0.065	0.0000	-0.039	-0.714	-0.046	0.033
0.95	-0.675	0.018	0.036	0.0000	-0.024	-0.788	-0.029	0.022
1.00	-0.750	0.003	0.006	0.0000	-0.004	-0.864	-0.005	0.004
Σ	-----	-----	3.6569	0.0154	0.415	0.000	0.445	0.445

$$\begin{aligned}
 C &= 1.5 \text{ ft} \\
 I_x &= 0.0012 \text{ ft}^4 \\
 I_y &= 0.274 \text{ in}^4 \\
 I_{xy} &= 24 \text{ in}^4 \\
 I_y &= 0.033 \text{ ft}^4 = 692 \text{ in}^4 \\
 I_{xy} &= 0
 \end{aligned}$$

Actually, the moments of inertia around these axes are needed but with the section rotated through an angle equal to the pitch angle. If the new coordinates are denoted by x' and y' .

$$x' = X \cos \phi - y \sin \phi$$

$$y' = X \cos \phi + y \cos \phi$$

The desired moments of inertia $I_{x'}$ and $I_{y'}$ are expressible in terms of the previously calculated I_x , I_y , and I_{xy} .

$$\begin{aligned} I_{x'} &= A y'^2 dA \\ &= A (x \sin \phi + y \cos \phi)^2 dA \\ &= A x^2 \sin^2 \phi + y^2 \cos^2 \phi + 2xy \sin \phi \cos \phi dA \\ I_{x'} &= I_y \sin^2 \phi + I_x \cos^2 \phi + 2 I_{xy} \sin \phi \cos \phi \end{aligned}$$

Similarly,

$$I_{y'} = I_y \cos^2 \phi + I_x \sin^2 \phi - 2 I_{xy} \sin \phi \cos \phi$$

The loading is also computed with the section at the pitch angle ϕ . In this position the force normal to the x' - axis at a given value of r/R is:

$$Y_i = 0.1 w R c_i \cos \phi_i$$

where w is the loading per unit area and c_i is the corresponding chord length. The force parallel to the x' - axis is:

$$X_i = 0.1 w R c_i \sin \phi_i$$

The moments that these forces exert on each section are tabulated in Table D-5 for an ice crushing stress $w = 300$ psi. A_d and A , are the outboard projected areas; r_d and r , are the radial locations of the centroid of the respected areas.

The maximum tensile stress will occur at the leading or trailing edge depending on whether the ice is pressing through the blade from the forward or aft side of the screw. If z denotes the maximum distance from the centroid to the leading or trailing edge parallel to the chord,

$$Z_b = (C/2 + \bar{x}) \sin \phi$$

when computing the stresss due to the moment M_d and

$$Z_l = (C/2 + \bar{x}) \cos \phi$$

when dealing with M_l . The stress is given by:

$$\sigma = \frac{Mz}{I}$$

Table D-6 gives a tabulation of the final stresses: σ_d due to M_d and σ_l due to M_l .

TABLE D-6 ICE CRUSHING STRESSES

r/R	σ_d (psi)	σ_l (psi)
0.4	30300	12000
0.6	18600	5600
0.8	8800	2900

The ice deflection strut is a beam fixed at both ends. Roark (1954) gives the moment as $1/8 wl$ where the length is taken as $l = 6' = 72$ in and the loading per foot is $300 \text{ psi} * 1.5' * 12'' = 6400 \text{ lbs/in}$.

Hence,

$$M = 1/8 6400 \text{ lbs/in} * 72 \text{ in} = 57,600 \text{ in/lbs.}$$

The stress is given by:

$$\sigma = \frac{M Y_u \max}{I_x} = \frac{57,600 \text{ in/lb} * 0.27 \text{ ft} * 12''}{24 \text{ in}^4}$$

or

$$\sigma = 7780 \text{ psi}$$

TABLE D-5 ICE CRUSHING MOMENTS ON BLADE

r/R	c (ft)	ϕ (deg)	$c \cos\phi$ (ft)	r (ft)	$rc \cos\phi$ (ft 2)	A_d (ft 2)	r_d (ft)	M_d (in lb)
0.3	3.200	24.79	2.905	1.275	3.704	11.74	2.864	9,671,000
0.4	3.607	22.38	3.335	1.700	5.670	10.42	3.037	7,220,000
0.5	3.929	20.23	3.687	2.125	7.834	8.92	3.224	5,082,000
0.6	4.098	18.98	3.875	2.550	9.882	7.32	3.417	5,289,000
0.7	4.475	17.66	4.264	2.975	12.686	5.59	3.617	1,858,000
0.8	4.645	16.63	4.451	3.400	15.132	3.73	3.827	827,000
0.9	4.474	16.70	4.285	3.825	16.391	1.88	4.044	213,000
1.0	4.678	17.38	2.275	4.250	9.669	--	--	--

r/R	$c \sin\phi$ (ft)	$rc \sin\phi$ ft 2)	A_1 (ft 2)	\bar{r}_1 (ft)	M_1 (in lb.)
0.3	1.342	1.71	4.004	4.109	8,528,000
0.4	1.373	2.33	3.427	3.547	6,302,000
0.5	1.359	2.89	2.846	2.980	4,397,000
0.6	1.333	3.40	2.274	2.410	2,841,000
0.7	1.358	4.04	1.703	1.905	1,681,000
0.8	1.329	4.52	1.132	1.554	912,000
0.9	1.286	4.92	0.576	1.815	542,000
1.0	0.712	3.03	--	--	--

INITIAL DISTRIBUTION LIST

	<u>No. of Copies</u>
Commandant U. S. Coast Guard Washington, D.C. 20563	6
Defense Documentation Center Cameron Station Alexandria, Virginia 22314	20
Assistant Librarian Technical Processing Division U. S. Naval Academy Annapolis, Maryland 21302	4
Academic Dean U. S. Naval Academy Annapolis, Maryland 21402	1
Director of Research U. A. Naval Academy Annapolis, Maryland 21402	1
Division Director Division of Engineering and Weapons U. S. Naval Academy Annapolis, Maryland 21402	1
Department Chairman Naval Systems Engineering Department U. S. Naval Academy Annapolis, Maryland	2
Professor T. J. Langan U. S. Naval Academy Annapolis, Maryland 21402	3